

**Cldn2-Trpv6 Double Knockout Mice have Hypocalcaemia and Reduced Bone Mineral Density**

by

Harneet Bhullar

A thesis submitted in partial fulfillment of the requirements for the degree of

Master of Science

Department of Physiology  
University of Alberta

© Harneet Bhullar, 2023

## ABSTRACT

Central to calcium homeostasis and bone health is adequate intestinal calcium absorption. Calcium from the diet is absorbed via either a transcellular or a paracellular pathway both of which are regulated by calciotropic hormones. In cases of low dietary calcium availability, a transcellular pathway that relies at least in part on the apical calcium channel Trpv6 predominates. However, when calcium is abundant in the diet, paracellular calcium absorption occurs through tight junction proteins, including claudin-2 (Cldn2). This tight junction protein also plays a role in calcium reabsorption from the renal proximal tubule to help maintain overall calcium balance. Despite this, Cldn2 knockout mice only display mildly altered calcium homeostasis. Specifically, they have hypercalciuria without evidence of altered bone mineral density (BMD), plasma calcium or calciotropic hormone levels. Similarly, mice homozygous for a non-functional Trpv6 (TRPV6<sup>D541A/D541A</sup>) channel have reduced intestinal calcium absorption without altered urine or plasma calcium levels, yet only display reduced intestinal calcium absorption when fed a low calcium diet. We hypothesized that the lack of a more pronounced phenotype in these two murine models was due to the compensation of one pathway in the absence of the other. To test this hypothesis, we crossed claudin-2 knockout mice with mice expressing the mutant Trpv6, generating a functional double knockout (dko, Cldn2<sup>-/-</sup>/TRPV6<sup>D541A/D541A</sup> mice). The dko mice displayed hypocalcaemia and a significant renal calcium leak. In contrast to the single claudin-2 KO mice or single TRPV6<sup>D541A/D541A</sup> mutant animals the dko mice had elevated plasma calcitriol and parathyroid hormone. Moreover, BMD was reduced in the dko mice. RT-qPCR of intestinal segments and whole kidney revealed increased calbindin-D<sub>9k</sub> expression in the proximal colon (but not duodenum) and calbindin-D<sub>28k</sub> in the kidneys,

consistent with compensatory increased transcellular absorption from the colon and distal nephron. Together these results are consistent with the paracellular pathway compensating for the loss of transcellular calcium absorption from the intestine.

## PREFACE

This thesis is a part of a project; The role of transport proteins in Epithelial Sodium, Bicarbonate, Phosphate and Calcium Transport and Breeding Colonies, AUP00000213, which has received research ethics approval from the University of Alberta Research Ethics board.

Parts of Chapter 1 of this thesis was published as **Beggs MR, Bhullar H, Dimke H, Alexander RT**. The contribution of regulated colonic calcium absorption to the maintenance of calcium homeostasis. *The Journal of Steroid Biochemistry and Molecular Biology*. 2022;220

## ACKNOWLEDGEMENTS

I would like to start by thanking my colleagues that I've had the pleasure to work with over my last three years in this lab. Your support and guidance have been invaluable in getting me to the finish line. Among the amazing trainees I owe my thanks to are Kennedy Young, Rebecca Tan, Matthew Saurette, Tate MacDonald and Christy Lee. I am extremely grateful for the endless help and patience that our lab technicians, Wanling Pan and Debbie O'Neill, provided me with throughout my time in the lab. Next, I must extend my gratitude to my supervisor, Dr. Todd Alexander for giving me the opportunity to learn and grow as a scientist in a safe space. Thank you for fostering my curiosity and teaching me how to think and ask questions.

My committee members, Dr. Harley Kurata and Dr. Shereen Hamza, thank you for providing me with your feedback and sharing your immense knowledge with me. Your guidance and expertise have allowed me to complete my project successfully.

Lastly, I would also like to thank my family and friends for their support in this journey. Thank you for listening to my long presentations while I practiced despite having minimal knowledge of my topic! I would not have been able to get to where I am today without the support of every individual in my life outside of the lab.

## **Table of Contents**

### **CHAPTER 1: INTRODUCTION**

Calcium and its Physiological Relevance	2
Calcium Homeostasis Overview	2
Intestinal Calcium Absorption	9
Renal Calcium Reabsorption	14
Trpv6 Overview: Structure, Function and Relevance	23
Cldn2 Overview: Structure, Function and Relevance	31
Hypothesis and Rationale	34

### **CHAPTER 2: MATERIALS AND METHODS**

Ethics Approval and Animals	36
Metabolic Cage Studies	36
Urine and Serum Analysis	39
Real Time Quantitative Polymerase Chain Reaction	39
Micro Computed Tomography	42
Statistical Analysis	42

## **CHAPTER 3: RESULTS**

Trpv6 <sup>D541A/D541A</sup> Mice Display Hypocalcemia and Elevated Calcitriol Levels on A Normal Calcium Diet	44
Trpv6 <sup>D541A/D541A</sup> Female Mice Have Altered Claudin 2 Expression in the Duodenum	51
Cldn2-Trpv6 Dko Animals Have Reduced Body Weight, Hypocalcemia and Hypercalciuria	58
Cldn2-Trpv6 Dko Mice Show Altered Bone Microarchitecture	66
Cldn2-Trpv6 Dko Mice Demonstrate Intestinal and Renal Compensation, However This Appears to be Inadequate	68

## **CHAPTER 4: DISCUSSION**

Estrogen Acts as a Protective Measure in Trpv6 <sup>D541A/D541A</sup> Female Mice for their Overall Calcium Balance	79
Cldn2-Trpv6 Dko Mice Have Compensatory Increased Colonic Calcium Absorption	81
Alternative Paracellular Calcium Absorption Through Claudin-12	83
Future Directions	84
<b>REFERENCES</b>	87

## List of Tables

<b>Table 1.1</b> Summary table of different genetic knockout animals and their calcium phenotype	30
<b>Table 2.1.</b> Summary of Primers and Probes used for RT-qPCR	41
<b>Table 3.1:</b> TRPV6 <sup>D541A/D541A</sup> mice urine ion normalized to urine creatinine	47
<b>Table 3.2:</b> TRPV6 <sup>D541A/D541A</sup> mice 24-hour urine biochemistry	48
<b>Table 3.3:</b> TRPV6 <sup>D541A/D541A</sup> mice 24-hour ion excretions in feces normalized to food intake, presented as a percentage	49
<b>Table 3.4:</b> Cldn2-Trpv6 dko mice urine ion normalized to urine creatinine	62
<b>Table 3.5:</b> Cldn2-Trpv6 dko mice 24-hour urine biochemistry	63
<b>Table 3.6:</b> Cldn2-Trpv6 dko mice 24-hour ion excretions in feces normalized to food intake, presented as a percentage.	64



## List of Figures

<b>Figure 1.1</b> Summary of Calcium Homeostasis	8
<b>Figure 1.2.</b> Intestinal Calcium Absorption	13
<b>Figure 1.3</b> Proximal Tubule Calcium Reabsorption	16
<b>Figure 1.4</b> Thick Ascending Limb Calcium Reabsorption	19
<b>Figure 1.5</b> Distal Convoluted Tubule Calcium Reabsorption	22
<b>Figure 1.6.</b> General Claudin Structure	32
<b>Figure 2.1.</b> 72-hour Metabolic Cage Experimental Protocol	38
<b>Figure 3.1.</b> Summary of Metabolic Cage data of TRPV6 <sup>D541A/D541A</sup> Mice on a Normal Calcium Diet	45
<b>Figure 3.2.</b> TRPV6 <sup>D541A/D541A</sup> Male Mice have Hypocalcemia and Elevated Calcitriol levels	46
<b>Figure 3.3:</b> TRPV6 <sup>D541A/D541A</sup> female mice show a marked reduction in cldn2 expression in the duodenum.	52
<b>Figure 3.4:</b> TRPV6 <sup>D541A/D541A</sup> mice have unaltered gene expression of calcium absorption pathway genes in the jejunum.	53
<b>Figure 3.5:</b> TRPV6 <sup>D541A/D541A</sup> mice have unaltered gene expression of calcium absorption pathway genes in the ileum.	54
<b>Figure 3.6:</b> Gene expression in the proximal colon of TRPV6 <sup>D541A/D541A</sup> mice.	55
<b>Figure 3.7:</b> Kidney gene expression of various calcium absorbing pathway genes in TRPV6 <sup>D541A/D541A</sup> mice	56
<b>Figure 3.8:</b> Summary of Metabolic Cage data of Cldn2 <sup>-/-</sup> /TRPV6 <sup>D541A/D541A</sup> DKO Mice on a Normal Calcium Diet.	60

<b>Figure 3.9:</b> Cldn2-Trpv6 DKO mice have Hypocalcemia, Elevated PTH and Calcitriol levels and Hypercalciuria	60
<b>Figure 3.10:</b> Cldn2-Trpv6 dko animals altered bone microarchitecture and male animals have reduced cortical bone mineral density.	66
<b>Figure 3.11:</b> Cldn2-Trpv6 DKO mice mrna expression of the calcium absorption pathway genes in the duodenum	70
<b>Figure 3.12:</b> Cldn2-Trpv6 DKO mice mrna expression of the calcium absorption pathway genes in the jejunum.	71
<b>Figure 3.13:</b> Cldn2-Trpv6 DKO mice mrna expression of the calcium absorption pathway genes in the ileum.	72
<b>Figure 3.14:</b> Cldn2-Trpv6 dko animals have compensatory increased calbindinD <sub>9k</sub> expression in the proximal colon	73
<b>Figure 3.15:</b> Cldn2-Trpv6 dko animals display renal compensation	74
<b>Figure 3.16:</b> Kidney mrna expression of Cldn2-Trpv6 dko mice.	75

## **List of Abbreviations**

Cldn-2	Claudin 2
TRPV6	Transient Receptor Potential Vanilloid 6
PTH	Parathyroid Hormone
PTH1R	Parathyroid Hormone 1 Receptor
RANKL	Receptor Activator of Nuclear Factor Kappa B Ligand
iCa	Ionized Calcium
TRPV5	Transient Receptor Potential Vanilloid 5
Napi2a	Sodium Phosphate Cotransporter 2a
Napi2c	Sodium Phosphate Cotransporter 2c
PKC	Protein Kinase C
NCX	Sodium Calcium Exchanger 1
PMCa1b	Plasma Membrane Calcium ATPase
DBP	Vitamin D Binding Protein
VDR	Vitamin D Receptor
RXR	Retinoid X Receptor

FGF23	Fibroblast Growth Factor 23
CaSR	Calcium Sensing Receptor
ERK1/2	Extracellular Signal-regulated Kinase 1/2
SGK1	Serum/Glucocorticoid-regulated Kinase 1
FGFR	Fibroblast Growth Factor Receptor
Nhe3	Sodium Proton Exchanger 3
Calb9k	CalbindinD-9k
Calb28k	CalbindinD-28k
PT	Proximal Tubule
TAL	Thick Ascending Limb
DCT	Distal Convoluted Tubule
CNT	Connecting Tubule
ROMK	Renal Outer Medullary Potassium Channel
NKCC2	Sodium Potassium Chloride Cotransporter
HEK293	Human Embryonic Kidney cells

## **CHAPTER 1: INTRODUCTION**

## CALCIUM AND ITS PHYSIOLOGICAL RELEVANCE

Calcium, the fifth most prevalent mineral present in the human body, plays diverse roles and has interactions with multiple organ systems.<sup>(1)</sup> Some of these roles include propagating heart and muscle contractions, nerve signal conduction, intercellular signaling and maintaining bone integrity. Ninety-nine percent of calcium bonds with phosphate to form hydroxyapatite and these crystals are then deposited into bone.<sup>(2)</sup> This calcium deposition early in life is crucial for maintaining bone integrity later in life.<sup>(1,3,4)</sup> The remaining 1% is available to carry out physiological roles. Disruptions in homeostatic levels of calcium can lead to adverse effects on the human body. A decrease in overall availability of calcium has detrimental effects on bone health and in young children can lead to the development of osteopenia whereas osteoporosis is commonly observed in postmenopausal women.<sup>(1,5-7)</sup> Due to its wide role in the body, calcium concentrations are tightly regulated in plasma by several different hormones including-parathyroid hormone (PTH), calcitonin and calcitriol (the active form of vitamin D), summarized in figure 1.1. These hormones work in conjunction with one another and are responsible for regulating the amount of calcium absorbed from the diet and reabsorption from the renal tubule.<sup>(8)</sup>

## CALCIUM HOMEOSTASIS OVERVIEW

### PARATHYROID HORMONE (PTH)

PTH is a polypeptide hormone that is synthesized as a preprohormone and undergoes various modifications before being released from the chief cells of the parathyroid gland as the active 84 amino acid peptide, in response to low plasma calcium.<sup>(9,10)</sup> Oxyphil cells also play a

minor role in PTH release and tend to increase in number with age and during some disease states such as in chronic kidney disease (CKD).<sup>(11)</sup> PTH is released in response to low calcium levels, and it directly targets the bones and kidney in order to raise plasma calcium levels. It also plays an indirect role in increasing intestinal calcium absorption. PTH has anabolic and catabolic effects on bone remodeling. PTH binds its receptor PTH1R on osteoblasts, which is a G protein coupled receptor that activates the cAMP mediated pathway.<sup>(12)</sup> Signalling through this pathway results in secretion of various cytokines and bone resorbing proteases from the osteoblast.<sup>(9,11,13)</sup> RANKL is then responsible for osteoclast genesis which leads to bone resorption to eventually increase plasma calcium levels.<sup>(14,15)</sup> PTH binds its receptor in the kidneys, whereby it increases the expression of cyp27b1, the gene encoding the enzyme 1-alpha hydroxylase, in the proximal tubule. Cyp27b1 is then responsible for catalyzing the last step in the synthesis of calcitriol. Calcitriol has targeted effects on intestinal calcium and phosphate transporters to increase absorption from the diet.<sup>(12,16-18)</sup> Furthermore, through its actions in the proximal tubule, PTH downregulates the expression of phosphate transporters Napi2a and Napi2c. In doing so, renal reabsorption of phosphate is decreased thereby increasing urinary phosphate excretion.<sup>(18)</sup> Lastly, PTH also increases transcellular calcium reabsorption in the distal convoluted tubule by signaling through the PKC pathway to increase active reabsorption through the calcium channel Trpv5. Once inside the epithelial cell, calcium is bound by calbindin-D<sub>28k</sub> and then shuttled to the basolateral side of the cell where it is extruded into the blood via NCX1 and PMCa1b.<sup>(12,18)</sup>

## CALCITRIOL

Calcitriol, the active form of vitamin D, is a steroid hormone which plays a critical role in the maintenance of calcium homeostasis via targeted actions on the intestines, kidneys and bones.<sup>(19)</sup> Ultraviolet B (UVB) radiation catalyzes the formation of pre-vitamin D from 7 dehydrocholesterol in the skin. Thermal isomerization is then responsible for converting pre-vitamin D<sub>3</sub> into pro-vitamin D, whereby a shift of hydrogen from C19 to C9 is observed.<sup>(16,20,21)</sup> In order to become an active hormone, provitamin D<sub>3</sub> must undergo a series of hydroxylation steps in the liver and then the kidneys. In hepatocytes, provitamin D<sub>3</sub> is hydroxylated at C25 by 25-hydroxylase, a cytochrome P450 enzyme, resulting in 25-hydroxyvitamin D. The final hydroxylation step in the synthesis of calcitriol occurs in the renal proximal tubule.<sup>(16,20–22)</sup> This step is tightly regulated by levels of PTH and FGF23. In response to low blood calcium, PTH is released which increases expression of Cyp27b1, another cytochrome P450 enzyme. Cyp27b1 hydroxylates 25-hydroxyvitamin D at the C1 position, synthesizing 1,25 dihydroxyvitamin D<sub>3</sub> or calcitriol.<sup>(21,23,24)</sup> FGF23 and calcitriol act as inhibitors of this final step, i.e., they work to decrease the levels of calcitriol by activating cyp24a1, the gene encoding the enzyme 24-hydroxylase. This enzyme hydroxylates 1,25 dihydroxyvitamin D<sub>3</sub> at C24, which inactivates calcitriol. FGF23 suppresses Cyp27b1 expression which leads to a decrease in calcitriol production.<sup>(21,24)</sup> Circulating calcitriol, bound to vitamin D binding protein (DBP) is able to cross the plasma membrane of enterocytes and bind vitamin D receptor (VDR) in conjunction with RXR. This multi-subunit complex crosses the nuclear membrane to act as a transcription factor which increases the expression of the calcium channel Trpv6 in the duodenum and colon.<sup>(22,25–27)</sup>



Vitamin D Receptor (VDR) KO mice display a significant decrease in expression of Trpv6 in the duodenum, consistent with expression being dependent on calcitriol signaling.<sup>(28)</sup> Furthermore, calcitriol may also play a role in increasing paracellular calcium absorption via altering expression of claudin 2 and claudin 12.<sup>(29)</sup> In the distal convoluted tubule of the nephron, calcium is reabsorbed by Trpv5, which is also upregulated by vitamin D and its metabolites.<sup>(24,30)</sup> Specific effects of calcitriol on bone include increasing osteoblast mediated osteoclast differentiation to increase bone resorption.<sup>(21)</sup> Calcitriol perturbs bone mineralization by increasing pyrophosphates and osteopontin, molecules that normally bind hydroxyapatite crystals and prevent its deposition.<sup>(21,31)</sup> Calcitriol deficiency also leads to rickets and osteomalacia due to the crucial role calcitriol plays in endochondral ossification.<sup>(32,33)</sup>

## CALCITONIN

Calcitonin is a peptide hormone consisting of 32 amino acids that plays an important role in maintaining calcium homeostasis. The primary actions of calcitonin include lowering blood calcium levels via targeted action on the bones and kidneys. It is released from the C cells or parafollicular cells of the thyroid gland in response to hypercalcemia.<sup>(34,35)</sup> Calcitonin release is mediated through calcium binding to the Calcium sensing receptor (CaSR) on C cells.<sup>(36)</sup> In the bones, it works primarily by decreasing osteoclast mediated bone resorption and stimulating osteoblast dependant bone formation. Osteoclasts have a highly invaginated ruffled membrane that is rich in vacuolar type proton pumps. These pumps secrete high levels of acid and acid hydrolases into the immediate space surrounding the osteoclasts which results in bone breakdown.<sup>(37)</sup> In the presence of calcitonin, proton pumps are internalized, halting bone

resorption. Along with this, recent evidence suggests that osteoclasts can release Wnt10b which acts as a signaling molecule that increases osteoblast activity.<sup>(37,38)</sup> In the kidneys, calcitonin works to increase the excretion of various electrolytes including, sodium, chloride, potassium, and calcium.<sup>(35,37)</sup> Calcitonin plays a role in regulating levels of calcitriol by increasing its plasma level, which in turn works to decrease calcitonin levels in a feedback loop. Both calcitonin and calcitriol work together during pregnancy and lactation in order to maintain maternal bone mass.<sup>(36,39)</sup>

## FGF23

Fibroblast growth factor (FGF23) is a phosphotropic hormone that regulates the level of circulating phosphate but also has an indirect effect on blood calcium levels by targeting the production of calcitriol.<sup>(36)</sup> FGF23 is a 32 kDa protein that undergoes several posttranscriptional modifications before being released as an active hormone. Primarily synthesized and released by osteoblasts and osteocytes, it has effector functions in the kidneys in the presence of its coreceptor, Klotho.<sup>(40,41)</sup> FGF23 is released in response to elevated phosphate levels, it causes the sodium phosphate cotransporters (Napi2a, Napi2c) in the renal proximal tubule to be internalized and eventually degraded. This in turn decreases phosphate reabsorption from glomerular filtrate back into the blood. In the distal convoluted tubule, FGF23, signalling through the FGFR and its downstream regulators- ERK1/2 and SGK1, directly works to increase Trpv5 expression and therefore increase calcium reabsorption from the filtrate.<sup>(40-42)</sup> In the proximal tubule, FGF23 decreases the expression of cyp27b1 and stimulates the expression of cyp24a1, which combined works to decrease the production of calcitriol. This decrease in calcitriol decreases intestinal

calcium absorption and to a lesser degree absorption of intestinal phosphate. Furthermore, FGF23 acts to decrease PTH levels via a FGFR and klotho dependent pathway which also influences overall calcium balance.<sup>(41,43)</sup>

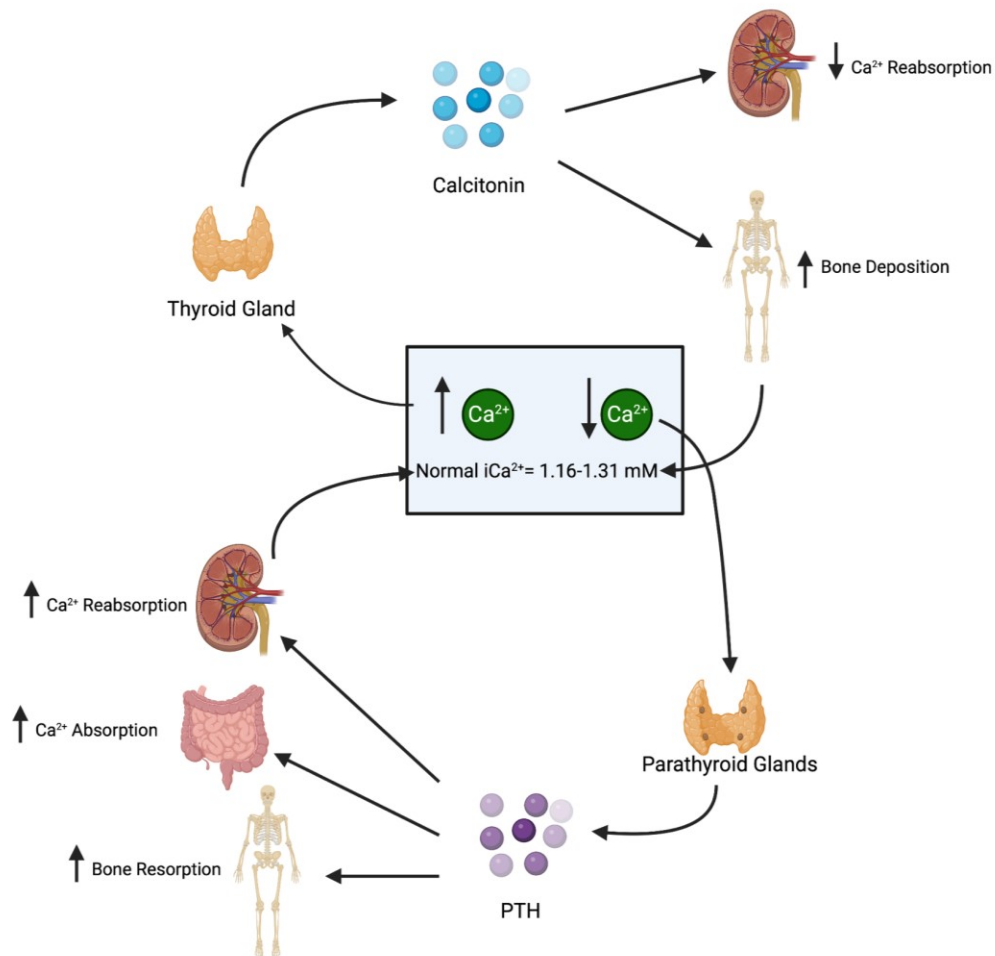


**Figure 1.1.** Summary of Calcium Homeostasis. Calcitonin is released in response to low plasma calcium levels. It acts on the kidneys to decrease calcium reabsorption and the bones to increase calcium deposition. PTH is released in response to low calcium levels. It works on the bones, intestines, and kidneys to increase plasma calcium levels. Normal plasma ionized calcium ( $iCa^{2+}$ ) is maintained between 1.16-1.31mmol/l. Created with BioRender.com

## INTESTINAL CALCIUM ABSORPTION

### PARACELLULAR CALCIUM ABSORPTION

A positive calcium balance in early life is essential for the development of healthy bones and growth later in life. Dietary calcium is the only new source of calcium in the body, therefore multiple ways of absorption in the intestines have evolved. Calcium absorption occurs through either a transcellular or a paracellular pathway.<sup>(3,44)</sup> The paracellular pathway relies on claudin tight junction proteins, and claudin-2 and 12 play a role in intestinal calcium absorption. Claudin 2 or 12 deletion in mice lead to adverse effects on calcium permeability across the intestines (Figure 1.2).<sup>(45,46)</sup> However, because the paracellular pathway relies on the electrochemical gradient this pathway can act as an absorption or secretory pathway depending on calcium availability and concentrations in the blood vs the intestinal lumen.<sup>(3)</sup> Paracellular calcium absorption is a passive process that accounts for the majority of calcium absorption under normal to high calcium availability. The driving force is hypothesized to be generated by two mechanisms, both of which rely on water movement. Nhe3, expressed on the apical side of intestinal epithelium cells allows for the active absorption of sodium in exchange of a proton. This transporter plays an important role in calcium absorption also, as Nhe3 null mice have perturbed calcium homeostasis.<sup>(47)</sup> Further interrogation for the role of Nhe3 in calcium homeostasis revealed that in Ussing chambers a Nhe3 inhibitor decreased net luminal to serosal calcium flux in the cecum of mice.<sup>(48)</sup> Absorption of sodium acts to generate a driving force for water absorption which results in a high concentration of luminal calcium. A high concentration of calcium can overcome the -5mV transepithelial potential difference across the intestines (lumen negative), allowing for paracellular calcium transport.<sup>(44,47,49)</sup> Another passive mechanism

of calcium absorption is solvent drag, the process whereby water movement moves ions through the tight junctions.<sup>(47,50)</sup>

The duodenum has the highest amount of calcium absorption when measured per unit length of intestine. However, due to the prolonged period of time spent in the jejunum and ileum, the overall majority of passive calcium absorption occurs here.<sup>(48,51)</sup> The colon also plays a role in overall calcium balance, where it can contribute either absorption or secretion of calcium.<sup>(3,46)</sup> Evidence from human studies revealed that overall calcium absorption is greatest when parts of the colon are conserved. Patients that underwent bowel resection, had greater net calcium absorption if their colon was intact compared to patients with a bowel resection with no colon.<sup>(52)</sup> In the colon, under conditions of high calcium availability calcium is secreted as evidenced by perfusion studies done on weight matched rats.<sup>(3)</sup> Recent evidence has shown that paracellular calcium flux is influenced by calcitriol, as exposing caco-2 cell lines to calcitriol alters expression of claudin 2 and claudin 12 therefore altering calcium permeability.<sup>(29)</sup> Furthermore, vitamin D receptor knock out animals show a reduction in claudin 2 and claudin 12 expression.<sup>(29,53)</sup>

## TRANSCELLULAR CALCIUM ABSORPTION

Transcellular calcium absorption is mostly observed under conditions of low dietary calcium availability. This pathway relies on calcium channels for uptake from luminal contents. Calcium entry into the enterocyte is mediated by Trpv6, and to some extent by the L type voltage channel, Cav1.3 as shown in figure 1.2.<sup>(44,54)</sup> Trpv6 and Cav1.3 have been proposed to have

complementary roles and their level of expression is reflective of that. Trpv6 expression is highest in the duodenum, and it tapers off distally. Cav1.3 expression follows the opposite trend. Trpv6 is active under hyperpolarizing conditions as occurs with fasting whereas Cav1.3 is activated during depolarizing conditions which are associated with digestion.<sup>(25,55)</sup> Once inside the cell, calcium is bound with high affinity to shuttle proteins known as calbindins (calb9k in the intestine, calb28k in kidneys).<sup>(53,56–58)</sup> Along with their role in ferrying calcium from the apical side of the cell to the basolateral side, calbindins also act to buffer calcium in the cell to prevent its toxic effects.<sup>(59)</sup> At the basolateral side, calcium is extruded from the cell into the blood via plasma membrane calcium ATPase (PMCa1b) and sodium calcium exchanger (NCX1).<sup>(53,58,60,61)</sup> PMCa1b works to extrude roughly 80% of calcium from the cell whereas NCX1 transports about the remaining 20% calcium.<sup>(56,62)</sup>

Study of calcium homeostasis in genetically modified mice has provided significant insight into intestinal calcium absorption. Calb9k null mice show no deficiencies in calcium homeostasis as they have comparable serum calcium levels to their WT littermates. They are also able to respond to calcitriol by increasing their intestinal calcium absorption, indicating that calb9k is not necessary for overall transcellular calcium absorption.<sup>(63)</sup> Interestingly, calb28k null mice display ataxia, however no perturbations in calcium homeostasis were evident.<sup>(64)</sup> PMCA1b, gene name Atp2b1, is essential to calcium absorption as complete deletion of PMCa1 is embryonically lethal in mice. Generating an intestine specific knockout of PMCa1 revealed that these mice are smaller in size at birth when compared to their WT littermates. Furthermore, these mice have a significant reduction in bone mineral density at 2 months of age and show a trend of lower serum calcium levels, although this was not significantly reduced. These animals also show a decreased response to exogenous calcitriol, as they fail to upregulate intestinal

calcium absorptions to the same extent as the WT littermates can.<sup>(65)</sup> NCX1 plays an important role in cardiomyocyte development, and NCX1 knockout in mice is embryonically lethal. Closer analysis revealed the formation of unorganized myofibrils and z lines when compared to WT littermates.<sup>(66)</sup> Therefore, studying the secondary role of NCX1 in calcium homeostasis has been difficult. Experiments with rabbit kidney cells have shown a role for NCX1 in extruding calcium from the cell into the blood across the basolateral membrane.<sup>(67)</sup> A role for Cav1.3 has been demonstrated in intestinal calcium absorption in mice. SGLT1 mediated glucose absorption causes local depolarization in the cell which opens Cav1.3 channels, allowing calcium entry into the cell.<sup>(55,68)</sup> Cav1.3 knock out male mice had a significant reduction in body weight and decreased bone mineral content. As a result, they exhibit a smaller skeleton when compared to their WT littermates.<sup>(69)</sup> Net transcellular flux is completely eliminated in the jejunum of Cav1.3 KO animals at P14, indicating that Cav1.3 along with Trpv6 play an important role in calcium absorption in young mice.<sup>(54)</sup>



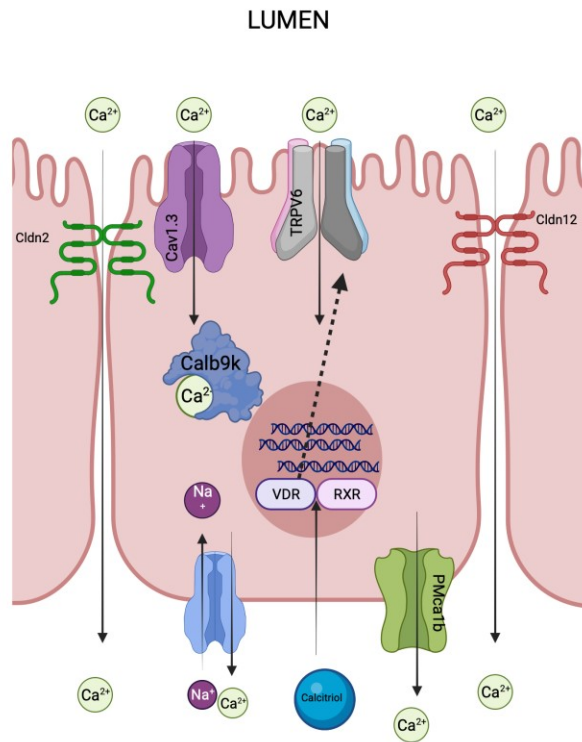


**Figure 1.2.** Intestinal Calcium Absorption. Calcium absorption is mediated transcellularly through Trpv6 and to some extent Cav1.3 and paracellularly through claudin-2 (Cldn2) and claudin-12 (Cldn12). Inside the cell, calcium is bound by calb9k, which shuttles it across the cell to the basolateral side. Calcium is moved across the basolateral membrane via either NCX1 or PMCA1b. In cases of low blood calcium, calcitriol is synthesized and released. It binds the Vitamin D receptor (VDR) and increases transcription of the TRPV6 gene which acts to increase intestinal calcium absorption. Created with BioRender.com

## RENAL CALCIUM REABSORPTION OVERVIEW

### MECHANISMS MEDIATING CALCIUM REABSORPTION IN THE PROXIMAL TUBULE

The smallest functional unit of a kidney, the nephron, is divided into multiple segments that have a myriad of effector functions which include blood pressure regulation, reabsorption of calcium, phosphate, water, sodium, and the elimination of waste.<sup>(12,70,71)</sup> Free ionized calcium is filtered at the glomerulus from the blood into the pro-urine. To prevent calcium wasting, the majority is reabsorbed along the nephron. 60-70% of calcium reabsorption occurs along the proximal tubule (PT). The thick ascending limb (TAL) is responsible for about 20-25% of reabsorption and lastly the distal convoluted tubule (DCT) reabsorbs the remaining 10-15%.<sup>(72-74)</sup> Defects in calcium reabsorption can cause several detrimental effects on the body such as hypercalciuria, rickets, and nephrocalcinosis.<sup>(74)</sup>

The paracellular pathway is responsible for the majority of calcium reabsorption that occurs in the PT. This pathway relies on the tight junction proteins claudins-2 and 12 that form pores allowing calcium reabsorption down its concentration gradient.<sup>(45,75)</sup> Some transcellular calcium reabsorption also occurs in the PT, however the mechanisms mediating this remain unclear.<sup>(74-76)</sup> The chemical gradient driving calcium reabsorption in the proximal tubule is generated via the actions of Nhe3, like in intestinal calcium absorption. Nhe3 actively moves sodium into the cell in exchange for a proton, water follows sodium movement into the cell increasing calcium concentration in the lumen. Calcium is then moved out of the lumen via the tight junction pores. The electrical gradient generated has also been hypothesized to drive calcium reabsorption. In the early PT, a lumen negative potential difference is generated by sodium coupled glucose transport. Along with this, bicarbonate is preferentially reabsorbed over

chloride, which creates a chloride concentration gradient. Chloride is then easily reabsorbed paracellularly, generating a lumen positive potential difference in the more distal PT. This lumen positive electrical gradient then allows for calcium reabsorption in the distal PT.<sup>(74,77)</sup> Claudin 2 and claudin 12 null mice have altered calcium permeability, resulting in defective calcium reabsorption in the PT. Furthermore, humans with inactivating claudin 2 mutations have evidence of kidney stone formation and significant hypercalciuria.<sup>(45,46,72,78)</sup> The PT is also the target of PTH, calcitonin, FGF23 and calcitriol. These hormones work together to maintain plasma calcium levels by targeting the expression of CYP27b1 which in turn regulates the synthesis of calcitriol.<sup>(42)</sup>

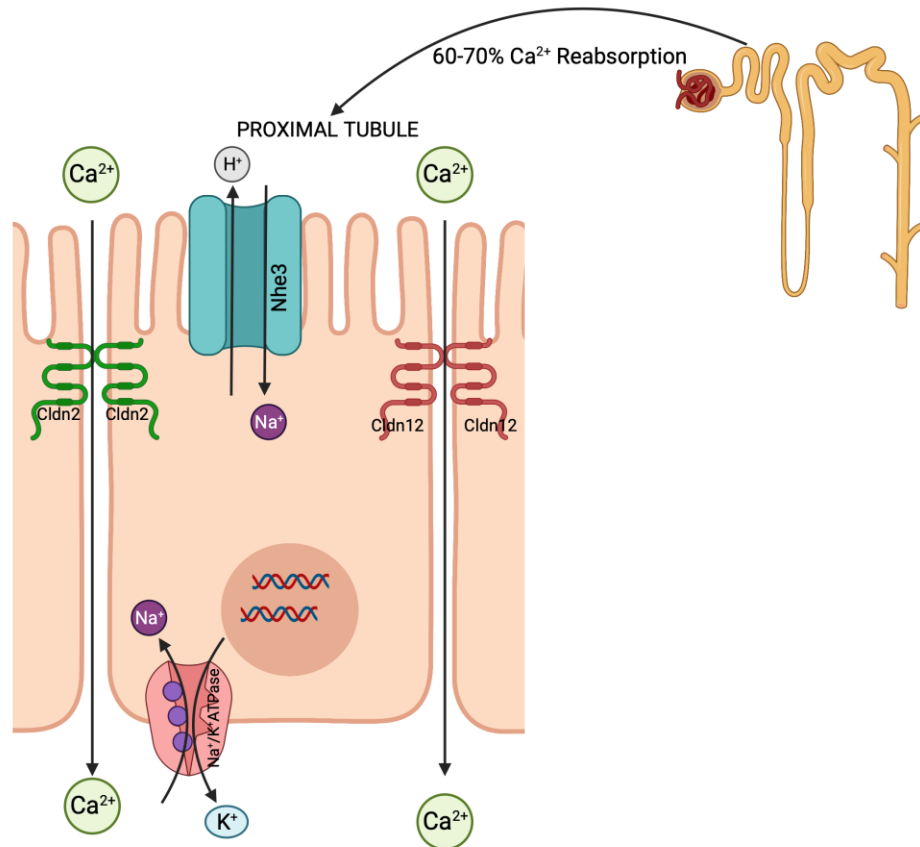


**Figure 1.3** Proximal Tubule Calcium Reabsorption. Calcium is freely filtered from the blood at the glomerulus. The majority of filtered calcium is reabsorbed from the proximal tubule through the tight junction proteins, claudin-2 (Cldn2) and claudin-12 (Cldn12). Paracellular calcium absorption is dependant entirely on the electrochemical gradients generated by a number of different ions. Created with BioRender.com

## MECHANISMS MEDIATING CALCIUM REABSORPTION IN THE THICK ASCENDING LIMB

The loop of Henle consists of the thin descending limb, thin ascending limb and lastly the thick ascending limb (TAL). Relative to the PT, the TAL is responsible for the next most amount of calcium reabsorption and this is a highly regulated process. The apical side of TAL epithelial cells contain a sodium potassium 2 chloride cotransporter (NKCC2) and the renal outer medullary potassium channel (ROMK). The NKCC2 is responsible for transporting 2 chloride ions, along with one sodium and one potassium into the cell. The ROMK channels then move the accumulating potassium back into the lumen, generating a net positive luminal potential difference. The sodium and chloride ions are transported into the blood via the Na/K ATPase and chloride channels at the basolateral side. The overall reabsorption of sodium and chloride creates a driving force enabling the movement of calcium through cln16 and 19 paracellularly.<sup>(74,79)</sup> Hypercalciuria and nephrocalcinosis, are clinical manifestations of Bartters syndromes (Types 1 and 2), which is caused by mutations in NKCC2 or ROMK. Their role in disease states highlights their importance in regulating calcium reabsorption.<sup>(80,81)</sup>

Calcium reabsorption in the TAL is regulated by the CaSR, which is present in the basolateral membrane. In the TAL, the CaSR is activated in response to elevated blood calcium levels.<sup>(82)</sup> Upon activation it signals to increase claudin 14 expression via a  $G_{q/11}$ -PLC-P38 pathway.<sup>(83,84)</sup> Claudin 14 inhibits divalent cation paracellular reabsorption by blocking the pore formed by claudin 16 and claudin 19 in the TAL. Claudin 16 allows for cation permeation whereas claudin 19 prevents the movement of anions. Together these tight junction proteins allow for the reabsorption of calcium and magnesium from the TAL.<sup>(74)</sup> Mutations in these genes

result in familial hypomagnesemia with hypercalciuria and nephrocalcinosis (FHHNC), a disease characterized by significant calcium and magnesium wasting.<sup>(75,85,86)</sup> In vivo studies with si-RNA knockdown for either claudin 16 or claudin 19 have shown that both proteins are required to form a cation permeable pore in the TAL. Furthermore, the knockdown of claudin 19 causes a loss of claudin 16 in the tight junctions and vice versa, altering calcium and magnesium reabsorption.<sup>(86)</sup>

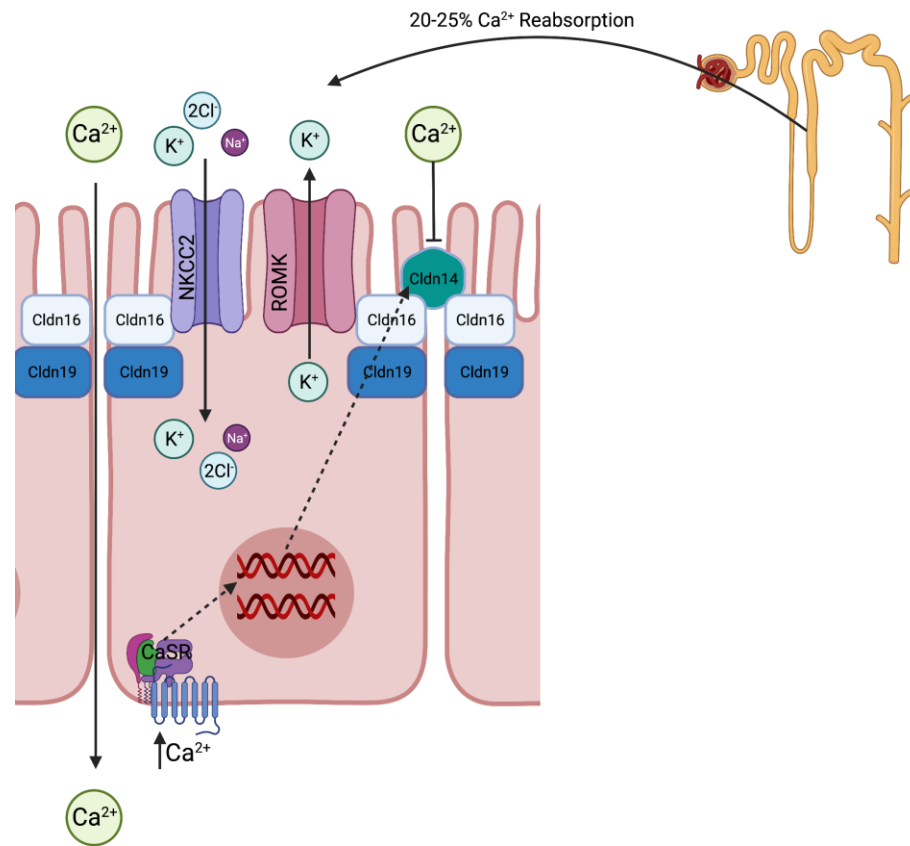


**Figure 1.4** Thick Ascending Limb Calcium Reabsorption. A lumen positive electrochemical gradient is generated by NKCC2 and ROMK. This gradient acts as the driving force for paracellular calcium reabsorption through claudin-16 (Cldn16) and claudin-19 (Cldn19). When blood calcium levels are elevated, signalling through the CaSR leads to expression of claudin-14 (Cldn14). Claudin-14 acts to block the pore formed by claudin-16 and claudin-19 and inhibit calcium reabsorption paracellularly.

Created with BioRender.com

## MECHANISMS MEDIATING CALCIUM REABSORPTION IN THE DISTAL CONVOLUTED TUBULE/CONNECTING TUBULE

The distal convoluted tubule and connecting tubule (DCT/CNT) are the most distal part of the nephron where any appreciable amount of calcium reabsorption has been observed. As it is the last part where reabsorption of calcium ions occurs, the DCT is critical in determining the final urine concentrations.<sup>(87)</sup> The mechanisms mediating calcium reabsorption at this site are predominately transcellular and occur in three steps. The first step is calcium entry into the cell through the apical calcium channel Trpv5, a homolog of Trpv6. The second step is calcium binding to shuttle proteins. Once calcium is in the cell, calb28k can then bind and ferry it towards the basolateral side where calcium is extruded via the combined actions of NCX1 and PMCa1b, which is the third step in the process.<sup>(74,79)</sup> The transcellular pathway is heavily affected by PTH and calcitriol which alter the expression of Trpv5.<sup>(12,42,74)</sup> Rats fed a deficient vitamin D diet show decreased expression of Trpv5 and Calb28k which was corrected by supplying the rats with vitamin D.<sup>(88)</sup> Studies with Trpv5 knockout mice show that complete ablation of Trpv5 causes the mice to experience significant hypercalciuria, along with an increase excretion of urinary phosphate. Furthermore, knockout mice have evidence of intestinal hyperabsorption of calcium as the levels of intestinal Trpv6 and calb9k are significantly upregulated, this is presumably to compensate for the renal leak. These animals also experience a significant reduction in trabecular and cortical bone thickness. This work provides support for the role of Trpv5 in calcium homeostasis.<sup>(89)</sup> A study has linked a single nucleotide polymorphism (SNP) in Trpv5 with kidney stone multiplicity in a Taiwanese population, providing evidence for a role of Trpv5 in contributing to nephrolithiasis.<sup>(90)</sup> FGF23 along with klotho regulate calcium reabsorption in the DCT. Signalling through this complex results in



Trpv5 trafficking to the plasma membrane which increases calcium reabsorption. Klotho, a beta-glucuronidase, hydrolyzes oligosaccharides on Trpv5 which causes Trpv5 to be confined to the plasma membrane. Co-expressing Trpv5 with klotho in HEK293 cells also led to an increase in  $^{45}\text{Ca}^{2+}$  flux, further implicating klotho in maintaining plasma calcium levels.(91)

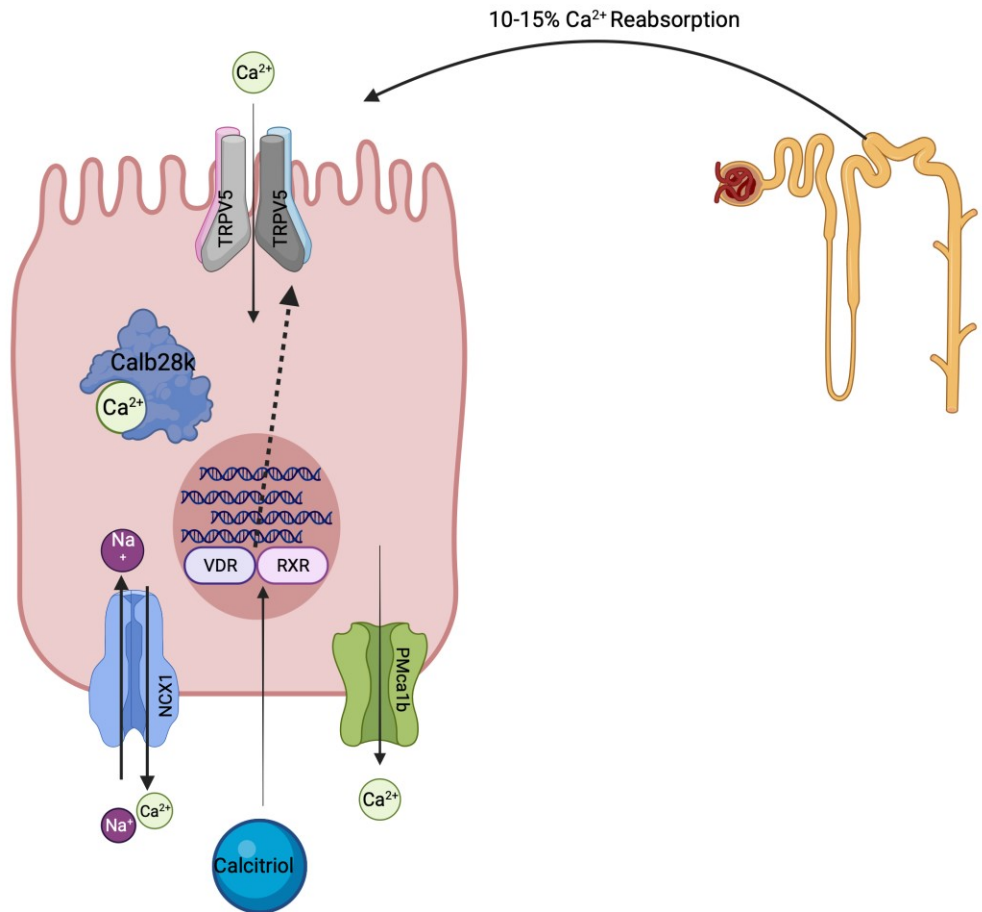


**Figure 1.5** Distal Convoluted Tubule Calcium Reabsorption. Active calcium reabsorption in the distal convoluted tubule and the connecting tubule. Calcium is actively reabsorbed through Trpv5, bound by calb28k and shuttles towards the basolateral membrane. At the basolateral membrane, calcium is extruded from the cell via the combined actions of NCX1 and PMCa1b. Trpv5 expression is increased by calcitriol.

Created with BioRender.com

## TRPV6 OVERVIEW: STRUCTURE, FUNCTION AND RELEVANCE

The transient receptor potential (TRP) superfamily is divided into six subcategories- TRPA, TRPP, TRPV, TRPM, TRPC, TRPML- all of which have a wide variety of physiological roles. These roles include sensory function, ion permeation, endothelial permeability, and smooth muscle proliferation.<sup>(92,93)</sup> Genetic variations in these channels also cause various diseases such as polycystic kidney disease, various cancers, and disrupted calcium homeostasis.<sup>(94)</sup> TRP channels have six transmembrane domains (S1-S6) with a pore loop between S5 and S6 and intracellular amino and carboxy terminals. TRPs can assemble in a homo or heterotetrametric formation to form ion permeable channels.<sup>(93,95)</sup> The extracellular portion of the pore confers cation selectivity. The carboxy terminus can be post translationally modified altering channel function and be involved with protein binding as well as assist with channel assembly.<sup>(96)</sup>

The TRPV sub family consists of a further six channels Trpv1-6 and these have a wide variety of roles. Trpv1-4 have relatively low cation permeability and instead function as heat activated chemosensory channels. Trpv5 and Trpv6 display 75% sequence homology and are the most calcium permeable channels with  $P_{Ca}/P_{Na} > 100$ .<sup>(92,93,96,97)</sup> Trpv5 is expressed mostly in the DCT of the kidneys, whereas Trpv6 expression has been observed in the intestines, kidneys, placenta, epididymis, exocrine tissue, and a few other sites.<sup>(8,97-100)</sup> Trpv6 has been implicated in active intestinal calcium absorption and along with calb9k expression increases significantly at the onset of weaning, when absorbing large amounts of calcium is crucial for growth.<sup>(58)</sup> The pore region between S5 and S6 determines the permeability of calcium. The aspartate at position

541 in Trpv6 and 542 in Trpv5 is responsible for calcium conductance through the channel.<sup>(101,102)</sup> There are several molecules regulating the opening and closing of these channels including PIP2, calcium binding proteins and intrinsic channel structure.<sup>(103)</sup> Trpv6 is transcriptionally regulated by calcitriol dependant gene activation, whereas faster non transcriptional alterations are achieved via the actions of calcium itself, calmodulin and interactions of Trpv6 with Annexin I/S100A11 post intracellular decrease of calcium.<sup>(103,104)</sup> Aberrations present in these proteins can lead to negative effects on the body as discussed above.

## TRPV6 KO MOUSE STUDIES

Due to its crucial role in active intestinal calcium absorption under low dietary calcium conditions, several studies with Trpv6 KO animals have been done to understand the effects of Trpv6 on whole body calcium homeostasis. Deletion of Trpv6 in mice results in a normal life span, however they experience developmental abnormalities early in life. KO animals kept on a regular (1%) calcium diet show a marked decrease in body weight that was not further exaggerated when switched to a low calcium diet (0.25%). Furthermore, fertility is significantly impacted as the KO animals tended to have fewer pregnancies and even fewer pups were born when compared to WT littermates. This work also showed that Trpv6 KO animals have a significant reduction in intestinal calcium absorption on either a normal or low calcium diet by measuring  $^{45}\text{Ca}^{2+}$  in serum after mice were administered  $^{45}\text{Ca}^{2+}$  orally. Furthermore, Trpv6 KO mice displayed significant hypercalciuria, and the animals also experienced elevated levels of PTH and calcitriol, presumably to compensate for the renal leak. Trpv6 KO mice have

significantly reduced femoral bone density which is not corrected by placing them on a high calcium diet.<sup>(105)</sup>

Benn et.al, reported a Trpv6-calb9k dko mouse model, in which no significant differences were observed in plasma calcium to wild-type mice, however a significant increase in PTH was detected.<sup>(58)</sup> Using everted gut sac assays to measure transcellular calcium absorption, they showed increases in intestinal calcium absorption *in vivo* when WT, Trpv6 KO, and calb9k KO mice were placed on a low calcium diet. Because the KO animals were able to increase intestinal calcium absorption (although not as much as the WT) this indicates that there may be other genes responsible for transcellular calcium absorption, the identity of which needs to be further interrogated.<sup>(58)</sup> A role of Trpv6 has been suggested in conditions of low dietary calcium availability. On a normal calcium diet, the loss of trpv6 has no effect on bone remodeling or bone mass as the KO mice had normal osteoid abundance and thickness. On a low calcium diet, both the WT and the KO animals had a reduction in bone mass, however the loss was comparable between the groups. The KO animals do have evidence of increased bone turnover and they had elevated osteocalcin levels indicating an increase in osteoblast activity.<sup>(57)</sup> Another group reported a severely affected bone microarchitecture environment in the KO mice with a significant increase in osteoclast activity. Cell culture studies also indicate an increase in bone resorbing osteoclasts cells when Trpv6 KO and WT bone marrow cells were cultured with the osteoclast producing ligands- M-CSF and RANKL.<sup>(106)</sup> Trpv6 has high expression in the trophoblasts and syncytiotrophoblasts where expression peaks when fetal bone mineralization is highest. Trpv6 KO fetuses have reduced calcium flux which potentially contributes to the reduced ash weight of the fetus.<sup>(107,108)</sup>

## TRPV6<sup>D541A/D541A</sup> MUTANT MOUSE STUDIES

Trpv6's ability to permeate calcium is dependant entirely on an aspartate at position 541 in rodents, alterations to this residue result in abrogation of channel function. The negatively charged aspartate in the pore region of the channel is responsible for calcium permeation, replacing this channel with an alanine residue results in a complete loss of channel function. Nilius et.al, showed when HEK293 cells were transfected with WT and mutant Trpv6, calcium permeability was abolished in the Trpv6 mutant cells.<sup>(109)</sup> A different group was able to show that Trpv6 channels are not constitutively open but are regulated by intracellular calcium concentrations. They were also able to confirm the complete loss of function of the mutant channels when expressed in HEK293 cells as no inward currents were detectable in whole cell patch clamp recordings.<sup>(110)</sup> A few studies done with genetic rodent models have been summarized in table 1.1.

Based on this in vitro model, a genetic knock in mouse model was generated with a non-functional Trpv6 channel. Weissgerber et.al, have shown impaired fertility in the Trpv6 mutant male mice. Trpv6 is expressed in the epididymis where it functions to actively absorb calcium. Mice expressing the Trpv6 pore mutation have impaired calcium absorption across the epididymis and as a result have abnormally high calcium levels in the caudal epididymal fluid. This results in deteriorating sperm motility which causes a significant reduction in the ability of the sperm to fertilize the egg. Like the Trpv6 KO mice, there was a significant reduction in litter size observed in mating between Trpv6<sup>D541A/D541A</sup> animals. Evidence indicates that on a normal calcium diet Trpv6<sup>D541A/D541A</sup> mice have no deviations from WT littermates, however when challenged with a low calcium diet they show impairments. Trpv6<sup>D541A/D541A</sup> mice have normal

serum calcium levels on a normal calcium diet, however both WT and mutant animals show a significant reduction in serum calcium levels on a low calcium diet. Mutant animals on a low calcium diet also show a reduction in body weight, when compared to mutant animals on a normal calcium diet. Urinary calcium excretion was not altered in mutant mice on either diet. On a low calcium diet, Trpv6<sup>D541A/D541A</sup> mice are able to increase intestinal calcium absorption however less so than their WT littermates. When deprived of calcium, both WT and mutant mice also show significantly increased 1-alpha hydroxylase expression in the kidney, which works to synthesize active vitamin D production. Van der Eerden and colleagues have shown that mutant mice have comparable bone mass and microarchitecture as their WT littermates. They did note a reduction in bone size as femoral length, femoral head and cortical bone was reduced in the mutant animals. Contrary to the Trpv6 KO bone phenotype, this group concluded that although Trpv6 is expressed in bone cells it does not significantly affect bone metabolism.<sup>(106,111)</sup> Mutant animals show a reduction in net calcium flux across the duodenum at two months of age when measured with Ussing chamber studies. A reduction in calcium flux was also noted upon addition of ruthenium red, an ion channel blocker.<sup>(54,112)</sup> In the jejunum, Trpv6 expression was highest at P14 and mutant animals at P14 showed a significant decrease in calcium absorption indicating that Trpv6 is crucial in intestinal calcium absorption at this age. At P14, Trpv6<sup>D541A/D541A</sup> pups showed no significant differences in trabecular and cortical bone parameters, consistent with other calcium absorption pathways having a larger role at this age.<sup>(54)</sup>

## TRPV6 HUMAN DISEASE STATES

Trpv6 channels are expressed in a wide variety of tissues with varying functions and roles, as a result they are also involved in causing a number of disease states in humans. Trpv5 and Trpv6 have been linked to causing absorptive hypercalciuria, potentially leading to kidney stone formation. In Iceland, a genome wide association study linked a Trpv5 variant, L530R, to causing recurrent kidney stone formation.<sup>(113)</sup> A study done with patients from Switzerland revealed a higher frequency of a Trpv6 gain of function haplotype in individuals that form recurrent kidney stones. Mutations in Trpv6 have also been linked to defects in maternal fetal calcium transport, resulting in transient neonatal hyperparathyroidism. These mutations have been hypothesized to affect Trpv6 localization to the plasma membrane which decreases calcium absorption across the placenta.<sup>(108,114)</sup>

Alterations to Trpv6 function have recently been shown to play a role in chronic pancreatitis in certain populations. The onset of chronic pancreatitis in these individuals can be exacerbated by defective calcium homeostasis as a result of loss of function mutations in Trpv6, which is also expressed in the pancreas.<sup>(115,116)</sup> Estrogen is known to regulate expression levels of Trpv6 and a decline in estrogen levels has been linked to reduced expression of Trpv6 in postmenopausal women. This decrease in Trpv6 expression can contribute to osteoporosis.<sup>(117)</sup> Trpv6 has been linked to issues of male fertility and development of preeclampsia in pregnant women.<sup>(108)</sup> Trpv6 over expression has been linked with various cancers such as prostate, breast, thyroid, colon, and ovarian. Furthermore, over expression of Trpv6 has also been hypothesized to cause tumor aggressiveness. It has been reported that Trpv6 channel activity causes influx of calcium which suppresses IGF-1 mediated signaling to maintain cell quiescence. As a result,



chronic entry of calcium causes epithelial cells to come out of their quiescence and start cell division, leading to tumour development in epithelial cells.<sup>(118)</sup>

<b>Genetic Models</b>	<b>Serum Calcium</b>	<b>Urine Calcium</b>	<b>Fecal Calcium</b>	<b>Calcitriol</b>	<b>PTH</b>	<b>Bone phenotype</b>
<b>Calb9k KO</b>	Normal	Normal	Normal	Normal	Normal	Normal <sup>(119)</sup>
<b>Calb28k KO</b>	Normal	Normal	Normal	Normal	Normal <sup>(120)</sup>	Reduced total and cortical BMD <sup>(121)</sup>
<b>Trpv5 KO</b>	Normal	Hypercalciuria	Hyperabsorption of calcium	Elevated	Normal	Reduced trabecular and cortical thickness <sup>(89)</sup>
<b>Trpv6 KO</b>	Normal	Hypercalciuria	ND	Elevated but not significant	Elevated	Not changed on normal calcium diet (58,105)
<b>Trpv6<sup>D541A/D541A</sup></b>	Normal	Normal	ND	ND	ND	Not changed <sup>(111)</sup>
<b>CLDN2 KO</b>	Normal	Hypercalciuria	Increased	Normal	normal	Normal <sup>(46)</sup>
<b>CLDN12 KO</b>	Normal	Normal	Normal	Normal	Normal	Normal <sup>(78)</sup>
<b>Cldn2/12 dko</b>	Hypocalcaemia	Hypercalciuria	Increased	Not significantly increased	increased	Reduction in trabecular and cortical BMD <sup>(45)</sup>

**Table 1.1** Summary table of different genetic knockout animals and their calcium phenotype.

ND: Not determined.

## CLAUDIN 2: STRUCTURE, FUNCTION AND RELEVANCE

Tight junctions play a role in cell adhesion, conferring selective ion permeability in epithelial and endothelial cells. Claudin proteins are tight junction proteins that play a role in passive paracellular (re)absorption of various ions in the intestines and kidneys and also form a protective barrier.<sup>(122,123)</sup> They are 21-23 kDa in size and have four transmembrane domains (TM1-4) with an intracellular amino and carboxy terminus. Claudins also consist of 2 large extracellular loops and one short intracellular loop. The ion permeability is determined by the first extracellular loop which has been hypothesized to act as a selectivity filter whereas the second extracellular loop plays a role in mediating interactions with claudins in adjacent cells. Protein trafficking and stability is modulated by the carboxy terminus of claudin proteins.<sup>(75)</sup>

Claudin 2 functions in the intestines and kidneys to confer calcium permeability across the epithelium. Other claudins including claudin 12, 16, and 19 also play a role in maintaining calcium homeostasis.<sup>(75)</sup> Claudin 2 is highly expressed in the proximal tubule of the kidney where it plays a role in sodium reabsorption along with calcium. Selectivity in the pore region is determined by residues D65 and Y67, in the first extracellular loop of the protein, and their electrostatic interactions with cations. Along with playing a role in ion homeostasis, Claudin 2 is also known to play a role in cell proliferation and viability. As a result, elevated Claudin 2 expression has been altered in many disease states including gastric and colorectal cancer.<sup>(124)</sup> Due to its role in calcium reabsorption in the kidney, perturbations in *cldn2* expression cause a significant renal calcium leak thereby contributing to the formation of kidney stones.<sup>(45,46,125)</sup>

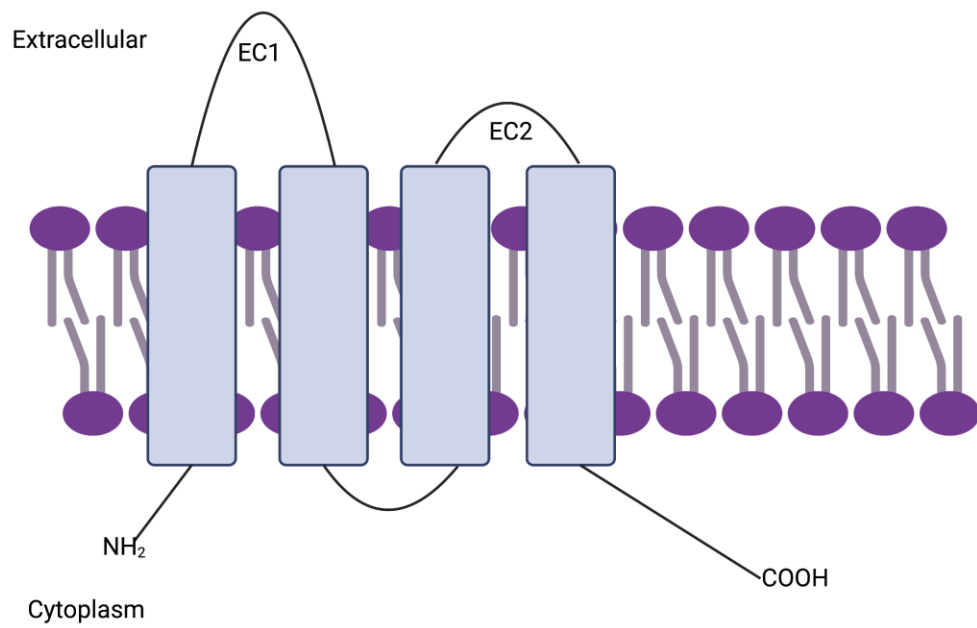


**Figure 1.6.** General Claudin Structure. Claudins are a family of tight junction proteins that confer selective ion permeability and play a role in calcium homeostasis. The structure consists of 2 extracellular loops, where EC1 confers ion permeability. Created with BioRender.com

## CLAUDIN 2 KO STUDIES

Studies with Claudin 2 knock out mice have shown that deletion of Claudin 2 results in significant hypercalciuria, but hypocalcaemia was not detected. This is attributed to defective proximal tubule calcium reabsorption in the absence of the Claudin 2 pore. The lack of a drop in serum calcium levels and the subsequent lack of elevated PTH and calcitriol was found to be due to a net increase in intestinal calcium absorption. BMD is unaltered in the KO animals.<sup>(46)</sup> Overall, Claudin 2 KO mice have normal growth, activity, and behaviour.<sup>(126)</sup> Curry et al. found that the KO animals had a reduction in colonic calcium permeability by mounting tissue in Ussing chambers and measuring calcium flux. Because claudins mediate paracellular absorption that is dependant entirely on the electrochemical gradient, they can also mediate secretion of ions. So, a net reduction in paracellular permeability indicates a decrease in net secretion which contributed to overall net increase in intestinal calcium absorption in the KO animals.<sup>(46)</sup> Von Kossa staining, and immunofluorescence revealed calcium deposits in the loops of Henle of the Claudin 2 KO animals mimicking the idiopathic hypercalciuria with kidney stone formation phenotype in humans. GWAS have also linked Claudin 2 mutations with increased risk of developing kidney stones.

Claudin 12 is expressed in the proximal tubule and plays a role in calcium reabsorption. Claudin 12 KO animals have comparable levels of serum and fecal calcium to WT animals. Perfusion of proximal tubules from Claudin 12 KO animals revealed a reduction in calcium permeability however the animals displayed no evidence of hypercalciuria.<sup>(78)</sup> The lack of a severe phenotype in the Claudin 2 and Claudin 12 KO mice was hypothesized to be due to compensation occurring by the other calcium permeable pathway. The deletion of both Claudin 2

and Claudin 12, to generate a dko mouse model provided insight into this. Claudin 2/12 dko mice had a significant calcium phenotype as they experience hypercalciuria, hypocalcaemia and a decrease in overall net calcium balance. In response to the reduction in serum calcium, hormonal compensation is evidenced by significantly elevated PTH levels. Increased PTH explains the significant decrease in trabecular and cortical bone mineral density in the dko mice. Taken together, these results indicate that both Claudin 2 and Claudin 12 are crucial in forming calcium permeable pores in order to maintain whole body calcium homeostasis.<sup>(45)</sup>

## HYPOTHESIS AND RATIONALE

Claudin 2 KO and Trpv6<sup>D541A/D541A</sup> mice on a normal diet do not have a significant calcium phenotype even though these proteins are responsible for the majority of paracellular and transcellular, calcium absorption respectively. Based on this observation we hypothesized that paracellular calcium absorption was compensating for the lack of transcellular calcium absorption in the TRPV6<sup>D541A/D541A</sup> mice and vice versa. To test this, we crossed TRPV6<sup>D541A/D541A</sup> mice with claudin 2 KO mice to generate a cldn2-trpv6 dko mouse model.

## **CHAPTER 2: MATERIALS AND METHODS**

## ETHICS APPROVAL AND ANIMALS

All animal experiments were approved by the University of Alberta Research Ethics Board animal ethics committee, Health Sciences section (AUP00000213). Claudin-2 knockout and TRPV6<sup>D541A/D541A</sup> mice were generated and maintained as previously described.<sup>(45,46,100)</sup> We generated Cldn2<sup>-/-</sup>/TRPV6<sup>D541A/D541A</sup> DKO mice by breeding cldn2 global KO animals with TRPV6<sup>D541A/D541A</sup> mutant animals. Animals were housed in a temperature and light controlled room whereby food and water were freely available. They were fed a standard rodent chow (Picolab Rodent Diet, 4% fat and 0.81% calcium). 72-hour metabolic cage studies were performed as previously described on 2–4-month-old mice<sup>(47,78,84)</sup>. For all experiments male and female animals were used, and all data presented displays the sex differences observed. Genotype of the animals was confirmed by polymerase chain reaction (PCR) as previously described.<sup>(46,100)</sup> Furthermore claudin 2 deletion was also confirmed by RT-qPCR in the intestines and kidneys.

## METABOLIC CAGE STUDIES

WT and DKO animals, aged 2-4 months, were placed in metabolic cages for 72 hours. Water and chow were provided *ad libitum*. Body weight was measured on Day 0, when the mice were placed in the metabolic cages. Every 24 hours, body weight measurements were taken along with urine and fecal weight. Urine pH was also measured every 24 hours. After 72 hours, mice were euthanized with a lethal dose of sodium pentobarbital. Blood was collected using cardiac puncture and stored in heparin coated tubes. Plasma and serum were separated by spinning at 3500rpm for 20 minutes at 4°C. Tissue was collected and snap frozen in liquid



nitrogen and stored at -80°C until required. Figure 2.1 summarizes the experimental protocol.

WT and TRPV6<sup>D541A/D541A</sup> mice were subject to the same protocol.

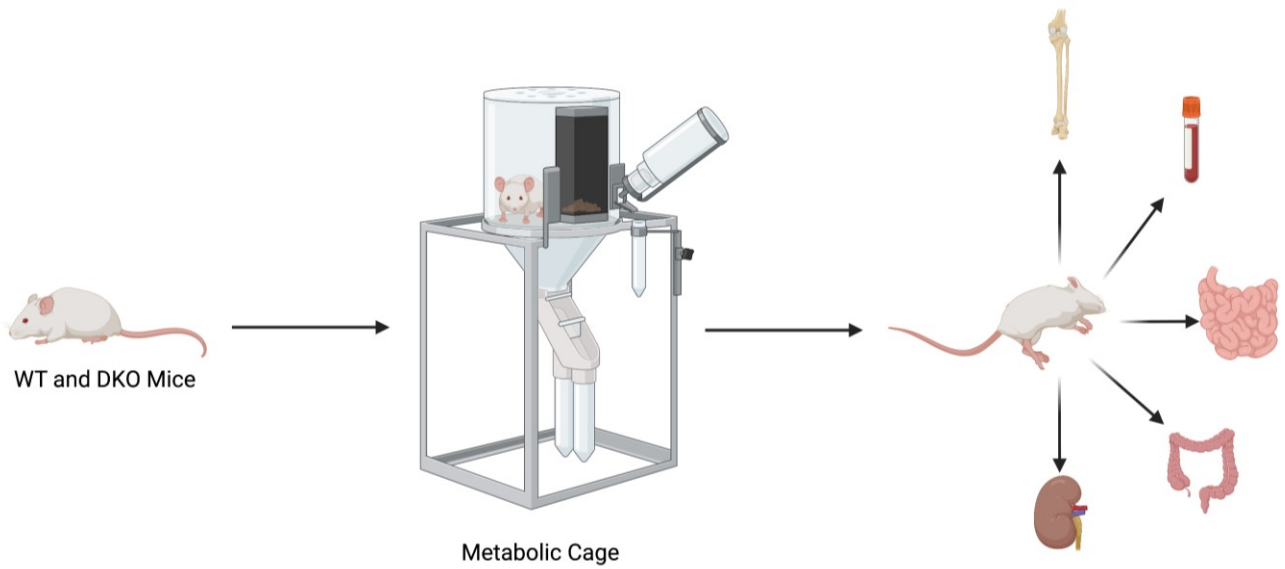


**Figure 2.1.** 72-hour Metabolic Cage Experimental Protocol. Animals were placed in metabolic cages for 72 hours and given water and chow *ad libitum*. Body weight measurements were taken on Day 0 and every 24 hours thereafter. Blood was collected via cardiac puncture, while the animal was under anesthesia. Post euthanizing, tissue was collected and snap frozen and then stored at  $-80^{\circ}\text{C}$ . Created with BioRender.com

## URINE AND SERUM ANALYSIS

Using an iSTAT1 Analyzer (Abaxis, Union City, CA, USA) with a CHEM8+ cartridge blood was assayed for electrolytes ( $\text{Na}^+$ ,  $\text{K}^+$ ,  $\text{Cl}^-$ ), including ionized calcium (iCa), glucose, urea nitrogen (BUN), hematocrit (Hct) and hemoglobin. Urine creatinine and electrolytes were measured via ion chromatography (Dionex Aquion Ion Chromatography system, Thermo Fisher Scientific Inc., Mississauga, ON, Canada). Urinary electrolytes were measured by ion chromatography. To determine cation concentration in urine and feces, 12 mM Methanesulfonic acid was used as an eluent and for anion, 4.5 mM  $\text{Na}_2\text{CO}_3$ / 1.5 mM  $\text{NaHCO}_3$  was used. The samples were diluted 1:50 with ddH<sub>2</sub>O and standard curves generated using 12 cation and 12 anion standards (Dionex, Thermo Fisher Scientific Inc., Mississauga, ON, Canada). Analysis was performed using Chromeleon 7 Chromatography Data System Software (Thermo Scientific). Serum collected was also used to measure the total amount of PTH (Immunotopics Mouse Intact PTH 1-84) and Vitamin D (Immunodiagnosics System Limited, UK) using ELISA.

## REAL TIME QUANTITATIVE POLYMERASE CHAIN REACTION

RNA extraction from tissue was performed as previously described.(45,54) Total RNA from frozen tissue was isolated using TRIzol reagent according to the manufacturer's instructions (Invitrogen, Carlsbad, CA, USA). 2  $\mu\text{g}$  from the isolated RNA was then made into cDNA (Thermo Fisher high-capacity cDNA Reverse Transcription Kit, CA, USA), following the manufacturer's instructions. All individual RNA samples were combined to make standards, that were used to make the standard curve for analysis. The cDNA, loaded in triplicate, was used to

determine mRNA expression of Cldn-2, -12, -15, -19, -16, -14, TrpV6, TrpV5, Calbindin-D<sub>9k</sub>, NCX, PMCa1b, SGLT1, Nhe3, Cav1.3, Trpm7, Calbindin-D<sub>28k</sub>, Cyp24 $\alpha$ 1 and Cyp27 $\beta$ 1 in different tissue using primers and probes (Integrated DNA technologies) as previously described and summarized in table 2.2.(47,127) Ezrin and 18S were used as controls to determine the fold change. A cq value greater than 35 was used as a cut off and considered not expressed in analysis. The expression levels were quantified with an ABI Prism 7900 HT Sequence Detection System (Applied Biosystems). Standard curve analysis was performed using a Quant Studio Design and Analysis Software version 2.4.3.

<b>Gene</b>	<b>Forward Sequence 5'→ 3'</b>	<b>Reverse Sequence 5'→ 3'</b>	<b>Probe Sequence 5'→ 3'</b>
<b>Cldn2</b>	AGGTGAGGGAAAT AGAAAAGCTAG	TGAGGGTAGAATGACTTT GGC	ATGGAGTGAAGGCAGAGATG AGAAGAGG
<b>Cldn12</b>	TCGCCAGAACGCAC TTC	TGAACTCAGATGCAACA GGAG	ATCCCGCTCACCCACTCCG
<b>Cldn15</b>	CTTCCCTACAAGCC TTCTACG	AGACAGTGGGACAAGAA ATGG	AGCTGATGTCACTCTCATCCG AGGT
<b>Cldn16</b>	AGACTGTTGGATGG TGAACG	AGCTTCAAGGGATGTTC TGC	CGCTTTTGATGGGATTCTGAAC CTGC
<b>Cldn19</b>	AAGGGCTGTGGATG TCTTG	CTCGTGCTGACTGGATAT GAC	AGGGCCAGGAGTGAATCGTA GAGT
<b>Cldn14</b>	TGGCATGAAGTTTG AAATCGG	CGGGTAGGGTCTGTAGG G	TGAGAGACAGGGATGAGGAG ATGAAGC
<b>Trpv6</b>	ATGGCTGTGGTAAT TCTGGG	AGGAAGAGTTCAAAGGT GCTG	AGAGGATCCCGATGAGCTGG GTC
<b>Calb9k</b>	TGGATAAGAATGG CGATGGAG	GCTAGAGCTTCAGGATT GGAG	ACAGCACCTACTGATTGAAC GCACG
<b>PMCalb</b>	CGCCATCTTCTGCA CCATT	CAGCCATTGCTCTATTGA AAGTTC	CAGCTGAAAGGCTTCCCGCC AAA
<b>Cyp24a1</b>	GGCGGAAGATGTG AGGAATATG	TCCTTTGGGTAGCGTGTA TTC	AGGGTCCGAGTTGTGAATGG CA

**Table 2.1.** Primers and Probes used for RT-qPCR

## MICRO COMPUTED TOMOGRAPHY

Tibia from WT and DKO animals were fixed in 4% formalin for three days and were then ethanol dried. The bones were then scanned using a Skyscan 1176 micro-computed tomography ( $\mu$ -CT) at a resolution of 18  $\mu$ m as previously described <sup>(45)</sup>. Reconstruction of the individual trabecular bone slices was done using NRecon. Data Analyser and CY Analyser were used to analyze the trabecular and cortical bone mineral density, trabecular number, trabecular and cortical thickness.<sup>(45,54)</sup> The region of interest consisted of 100 slices, starting at 20 slices below the metaphyseal growth plate. Voltage and current were set to 45 kV and 555  $\mu$ A respectively with a 0.5 mm Al filter with a 0.5 rotation step.

## STATISTICAL ANALYSIS

All statistical analysis was done using GraphPad Prism 9.0. Data were subject to a two-way ANOVA with Tukey's multiple comparison tests, unless otherwise stated. Data is presented as mean  $\pm$  SEM with outliers being removed by the ROUT method. A P value of less than 0.05 was considered to be statistically significant.

## **CHAPTER 3: RESULTS**

## TRPV6<sup>D541A/D541A</sup> MICE DISPLAY HYPOCALCEMIA AND ELEVATED CALCITRIOL LEVELS ON A NORMAL CALCIUM DIET

We first sought to confirm the calcium phenotype of the TRPV6<sup>D541A/D541A</sup> mutant animals on a normal calcium diet. Female WT and mutant animals had a lower body weight when compared to the male animals (Fig 3.1A). Over a 24-hour period both males and females had no significant differences noted in their chow or water consumption (Fig 3.1B and C). Urine volume voided by the TRPV6<sup>D541A/D541A</sup> showed no significant difference between genotypes and no sex differences were seen as well (Fig 3.1D). Similar results were observed for feces excreted over a 24-hour period by the animals (Fig 3.1E). This data indicates that the mutant animals are healthy overall and have no evidence of growth retardation as they have normal body weight when compared to their WT littermates.

In contrast with previously reported literature on TRPV6<sup>D541A/D541A</sup> mutant animals, we found that male mutant mice had significantly reduced plasma ionized calcium on a normal calcium diet whereas the female mutant mice had no discernable differences when compared to their WT littermates (Fig 3.2A). As a response to low blood calcium levels, we expected the mutant male animals to have elevated PTH and calcitriol levels. Male animals showed a trend towards increasing PTH levels whereas females no trend was observed (Fig 3.2B). Furthermore, blood calcitriol levels were significantly elevated, as expected, in the male mutant mice, but again no statistically significant differences were observed for the female mutant animals when compared to their WT littermates (Fig 3.2C).

Urinary calcium excretion in male mutant animals was not significantly different to their WT littermates whereas female mutant animals showed a significant reduction in calcium loss via the urine (Fig 3.2D). These values were normalized to creatinine to control for glomerular



filtration rate (GFR) which was not altered between the WT and mutant animals in either sex (Table 3.1). Additionally, urinary phosphate excretion was significantly elevated in the male mutant animals whereas no discernable differences were observed in female mutant animals when compared to their WT littermates (Fig 3.2E). We measured fecal calcium excretions normalized to the amount of chow consumed and we observed that intestinal calcium absorption was unaltered in the mutant animals regardless of the sex (Fig 3.2F). All other urinary ion excretions are summarized in Table 3.1. There were no significant differences between genotypes observed in  $\text{Mg}^{2+}$ ,  $\text{K}^+$ ,  $\text{Na}^+$ ,  $\text{Cl}^-$  in either male or female animals. Furthermore, no deviations from normal excretions of various ions was detected in either sex (Table 3.2).

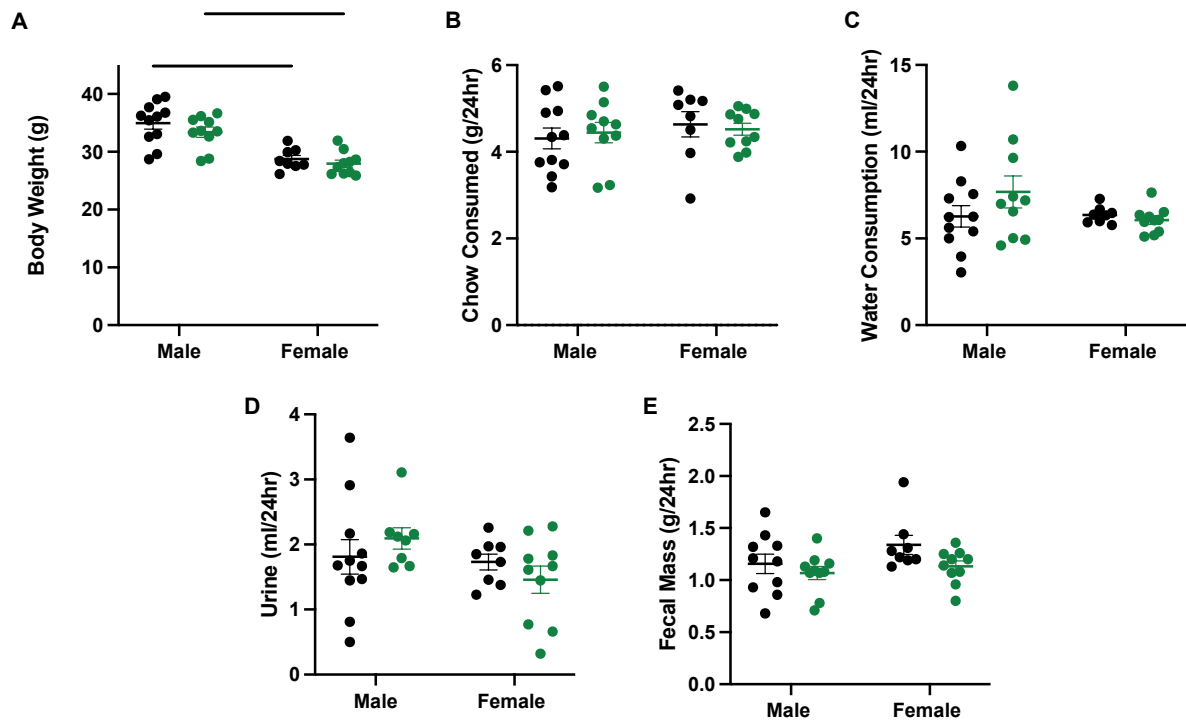


**Figure 3.1. Summary of Metabolic Cage data of TRPV6<sup>D541A/D541A</sup> Mice on a Normal**

**Calcium Diet.** (A) Day 3 body weight. (B) Chow consumption. (C) Water consumption. (D)

Urine volume voided. (E) Fecal mass excreted in 24 hours. n= 11 male WT, n= 8 male KO, n=8

female WT, n=10 female KO. Data is presented as mean ± SEM compared with a 2-way

ANOVA, Tukey's multiple comparison test. Black dots represent WT animals and green dots are

representative of TRPV6<sup>D541A/D541A</sup> Mice.

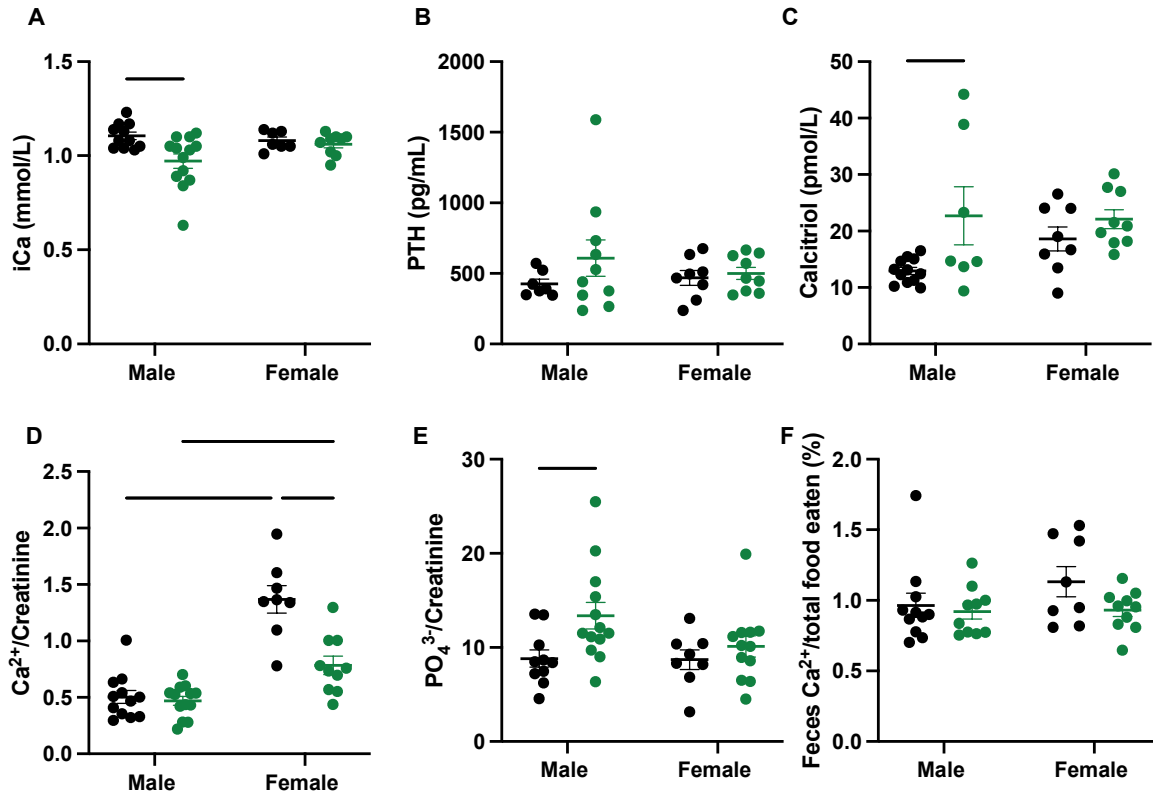


**Figure 3.2. TRPV6<sup>D541A/D541A</sup> Male Mice have Hypocalcemia and Elevated Calcitriol levels.**

(A) Blood iCa<sup>2+</sup>, n= 11 male WT, n= 10 male KO, n=7 female WT, n=9 female KO. (B) Serum parathyroid hormone level (PTH), n = 7 male WT, n= 10 male KO, n=8 female WT, n=10 female KO. (C) Serum calcitriol levels, n= 12 male WT, n= 7 male KO, n=8 female WT, n=9 female KO. (D) Urinary Ca<sup>2+</sup> normalized to creatinine, n= 12 male WT, n= 13 male KO, n=8 female WT, n=10 female KO. (E) Phosphate (PO<sub>4</sub><sup>3-</sup>) in urine normalized to creatinine, n= 10 male WT, n= 13 male KO, n=8 female WT, n=10 female KO. (F) Fecal Ca<sup>2+</sup> excretions calculated as a percentage of total chow consumed, n= 11 male WT, n= 10 male KO, n=8 female WT, n=10 female KO. All data is presented as mean ± SEM compared with a 2-way ANOVA, Tukey's multiple comparison test. Black dots represent WT animals and green dots are representative of TRPV6<sup>D541A/D541A</sup> Mice.

Urine Ion/ Creatinine	Male			Female		
	WT	KO	p-value	WT	KO	p-value
<b>Mg<sup>2+</sup></b>	6.53 ± 0.42	7.43 ± 0.71	0.396	9.51 ± 1.25	8.56 ± 0.89	0.818
<b>K<sup>+</sup></b>	117 ± 7.83	135 ± 16.7	0.319	153 ± 18.3	126 ± 11.5	0.488
<b>Na<sup>+</sup></b>	52.8 ± 2.90	62.0 ± 6.3	0.575	62.0 ± 6.7	50.1 ± 5.6	0.492
<b>Cl<sup>-</sup></b>	108 ± 6.8	129 ± 12.3	0.533	142 ± 18.1	116 ± 11.5	0.502
<b>PO<sub>4</sub><sup>3-</sup></b>	10.1 ± 1.12	13.3 ± 1.42	<b>0.045</b>	8.70 ± 1.03	8.82 ± 0.92	0.866

**Table 3.1: TRPV6<sup>D541A/D541A</sup> mice urine ion normalized to urine creatinine.** Data is presented as mean ± SEM. The results were compared using a 2-way ANOVA, Tukey's multiple comparison test.

24-hour Ion (mg)	Male			Female		
	WT	KO	p-value	WT	KO	p-value
<b>Ca<sup>2+</sup></b>	0.17 ± 0.02	0.11 ± 0.02	0.548	0.44 ± 0.06	0.26 ± 0.04	<b>0.005</b>
<b>Mg<sup>2+</sup></b>	1.34 ± 0.14	1.12 ± 0.20	0.778	1.72 ± 0.10	1.46 ± 0.18	0.991
<b>K<sup>+</sup></b>	38.1 ± 3.6	27.9 ± 4.6	0.215	44.7 ± 2.0	38.8 ± 3.5	0.773
<b>Na<sup>+</sup></b>	9.94 ± 0.88	7.42 ± 1.01	0.178	10.8 ± 0.59	9.07 ± 0.90	0.637
<b>Cl<sup>-</sup></b>	31.7 ± 2.9	24.5 ± 3.45	0.295	37.5 ± 1.89	32.5 ± 3.0	0.720
<b>PO<sub>4</sub><sup>3-</sup></b>	7.58 ± 0.81	6.76 ± 1.06	0.897	6.41 ± 0.83	6.53 ± 0.62	0.997
<b>Creatinine (mM)</b>	4.91 ± 0.39	3.25 ± 0.41	0.318	4.78 ± 0.59	5.84 ± 0.69	0.220

**Table 3.2: TRPV6<sup>D541A/D541A</sup> mice 24-hour urine biochemistry.** Data is presented as mean ± SEM. The results were compared using a 2-way ANOVA, Tukey's multiple comparison test.

	Male			Female		
	WT	KO	p-value	WT	KO	p-value
<b>Ca<sup>2+</sup></b>	0.965 ± 0.086	1.07 ± 0.17	0.576	1.13 ± 0.11	0.931 ± 0.166	0.079
<b>Mg<sup>2+</sup></b>	0.178 ± 0.011	0.171 ± 0.016	0.357	0.184 ± 0.015	0.143 ± 0.016	<b>0.025</b>
<b>K<sup>+</sup></b>	0.197 ± 0.017	0.195 ± 0.022	0.998	0.145 ± 0.017	0.176 ± 0.022	0.660
<b>Na<sup>+</sup></b>	0.081 ± 0.007	0.075 ± 0.009	0.968	0.091 ± 0.010	0.088 ± 0.009	0.998
<b>Cl<sup>-</sup></b>	15.4 ± 0.5	15.1 ± 0.3	0.986	17.8 ± 1.50	15.0 ± 1.92	0.060
<b>PO<sub>4</sub><sup>3-</sup></b>	1.27 ± 0.06	1.08 ± 0.09	0.395	1.44 ± 0.14	1.16 ± 0.21	0.154

**Table 3.3: TRPV6<sup>D541A/D541A</sup> mice 24-hour ion excretions in feces normalized to food intake, presented as a percentage.** Data is presented as mean ± SEM. The results were compared using a 2-way ANOVA, Tukey's multiple comparison test.

## TRPV6<sup>D541A/D541A</sup> MICE HAVE NO EVIDENCE OF INTESTINAL COMPENSATION

Due to the fact that we found only male mutant animals experience a significant drop in blood  $iCa^{2+}$  levels, we sought to uncover any potential compensatory upregulation of genes involved in calcium absorption. To this end, we measured mRNA expression of calcium transporting genes along the intestine and kidney. We observed a trend, that was not statistically significant, towards decreased mRNA abundance of claudin 2 in female mutant animals (Figure 3.3A). Claudin 2 forms a calcium permeable pore, which can act as both an absorption and a secretory pathway. This reduction in duodenal claudin 2 expression might occur to decrease calcium permeability thereby preventing the loss of calcium from blood into the intestinal lumen, protecting the female mutant animals from hypocalcemia. No other significant changes in mRNA expression were noted in the duodenum (Figure 3.3). qPCR performed on whole jejunum and ileum tissues did not detect significant differences in the mRNA abundance of *Cldn2*, *Cav1.3*, *NCX1*, *Trpv6*, *Calb9k* and *PMCA1b* (Figure 3.4A-F and C3.5 A-F) in either male or female mutant animals.

In the proximal colon, *Cav1.3* expression was significantly reduced in male mutant animals. (Figure 3.6C). *Cav1.3* has been hypothesized to contribute to transcellular calcium absorption. A significant reduction was also noted in the expression of *NCX1*, a transporter responsible for moving calcium from the cell into the blood (Figure 3.6E). No other significant changes were noted in either the male or female mutant animals.

Lastly, we sought to delineate compensation occurring in the kidneys of the mutant animals. We found an overall decrease in the expression of claudin 2 in both WT and mutant females when compared to their male counterpart (Figure 3.7B). *Cyp27b1* mRNA was

significantly upregulated in male mutant animals, presumably as a response to their low blood calcium levels. These results are consistent with the elevated levels of calcitriol in the mutant male animals (Figure 3.7E). Claudin 19 expression was increased in the female mutant animals when compared to male mutant animals. Claudin 19 contributes to calcium reabsorption in the TAL and may represent a compensatory pathway limiting urinary calcium excretion and reduced plasma calcium levels in the mutant female mice (Figure 3.7F).



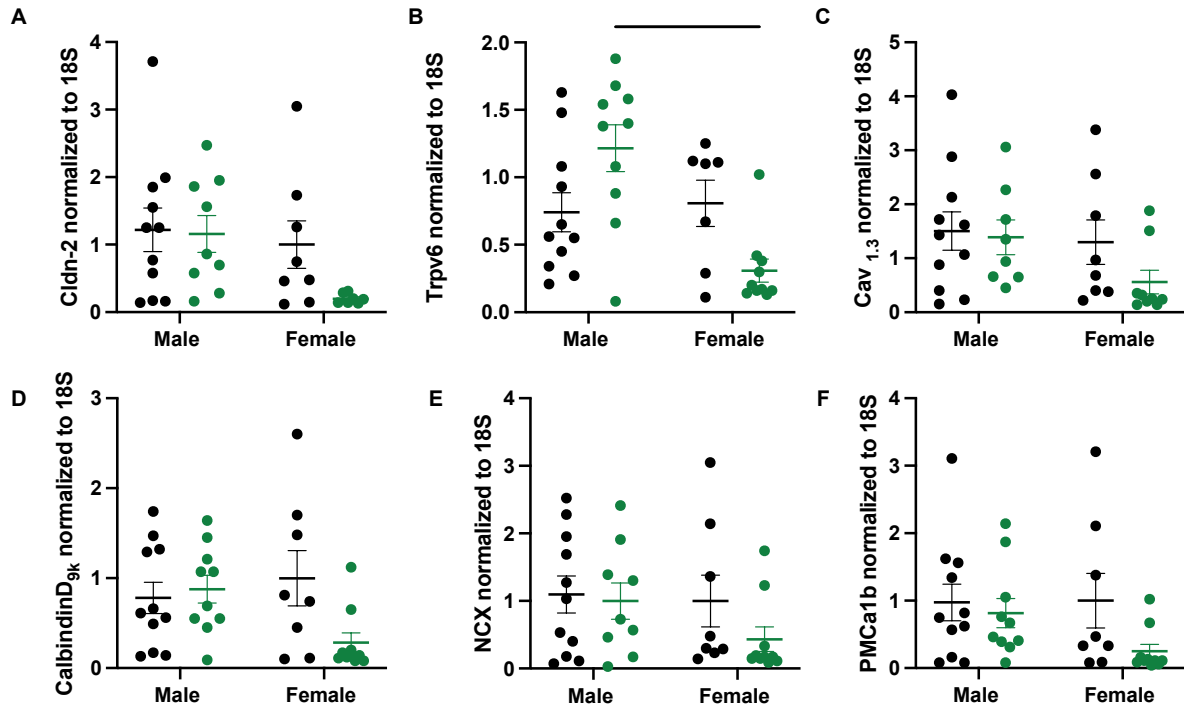


**Figure 3.3: TRPV6<sup>D541A/D541A</sup> female mice show a marked reduction in *cldn2* expression in the duodenum.** mRNA abundance of (A) *Cldn2*, (B) *Trpv6*, (C) *Cav1.3*, (D) *Calb9k*, (E) *NCX*, (F) *PMCa1b*. Results are normalized to 18S mRNA abundance. Data is presented as mean  $\pm$  SEM compared with a 2-way ANOVA, Tukey's multiple comparison. n= 10 male WT, n= 10 male KO, n=7 female WT, n=10 female KO. Black dots represent WT animals and green dots are representative of TRPV6<sup>D541A/D541A</sup> Mice.

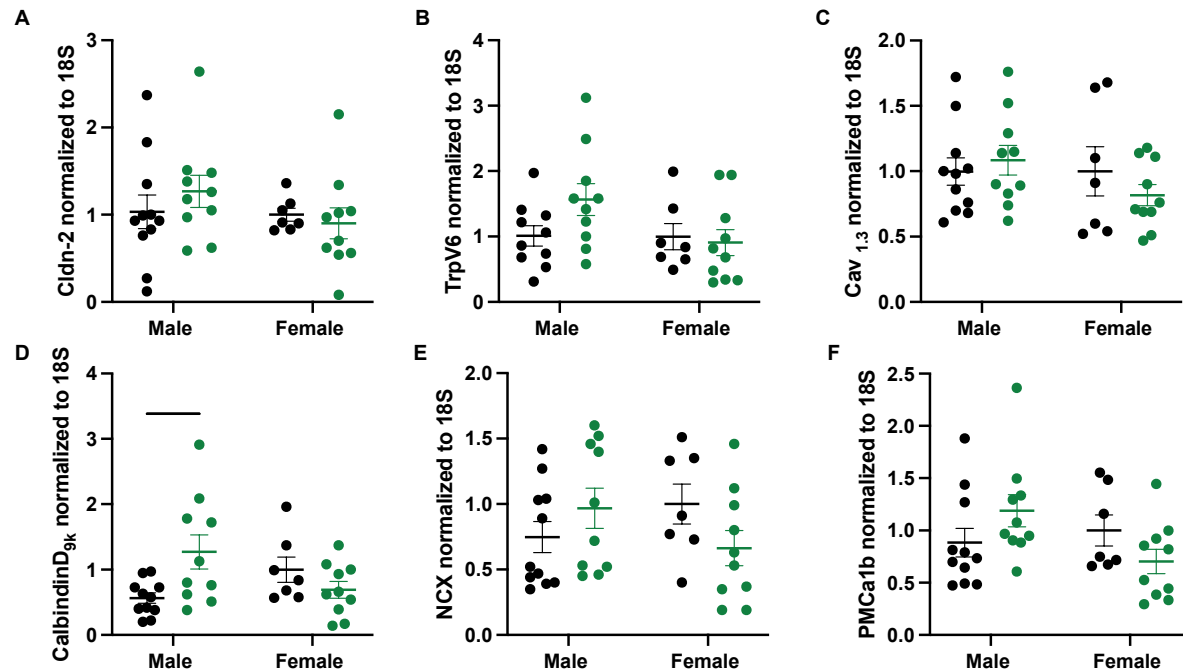


**Figure 3.4: TRPV6<sup>D541A/D541A</sup> mice have unaltered gene expression of calcium absorption pathway genes in the jejunum.** mRNA abundance of (A) *Cldn2*, (B) *Trpv6*, (C) *Cav1.3*, (D) *Calb9k*, (E) *NCX*, (F) *PMCa1b*. Results are normalized to 18S mRNA abundance. Data is presented as mean ± SEM compared with a 2-way ANOVA, Tukey's multiple comparison. Black dots represent WT animals and green dots are representative of TRPV6<sup>D541A/D541A</sup> Mice.

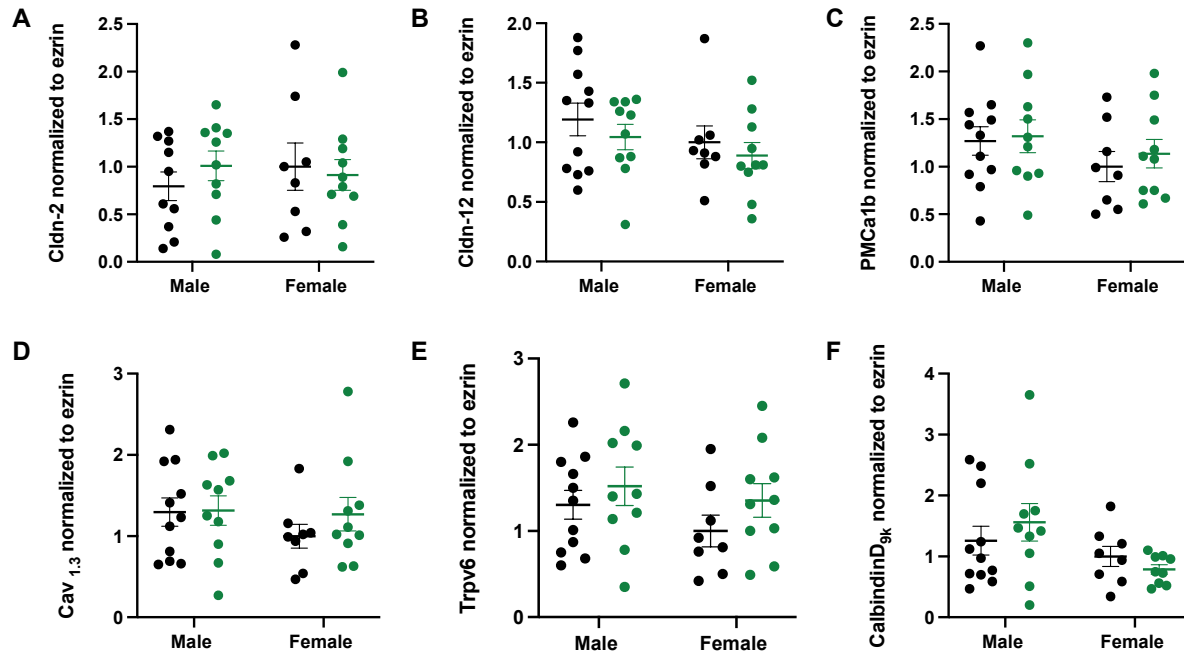


**Figure 3.5: TRPV6<sup>D541A/D541A</sup> mice have unaltered gene expression of calcium absorption pathway genes in the ileum.** mRNA abundance of (A) *Cldn2*, (B) *Cldn12*, (C) *PMCa1b*, (D) *Cav1.3*, (E) *Trpv6*, (F) *Calb9k*. Results are normalized to ezrin mrna abundance. Data is presented as mean ± SEM compared with a 2-way ANOVA, Tukey's multiple comparison. Black dots represent WT animals and green dots are representative of TRPV6<sup>D541A/D541A</sup> Mice.

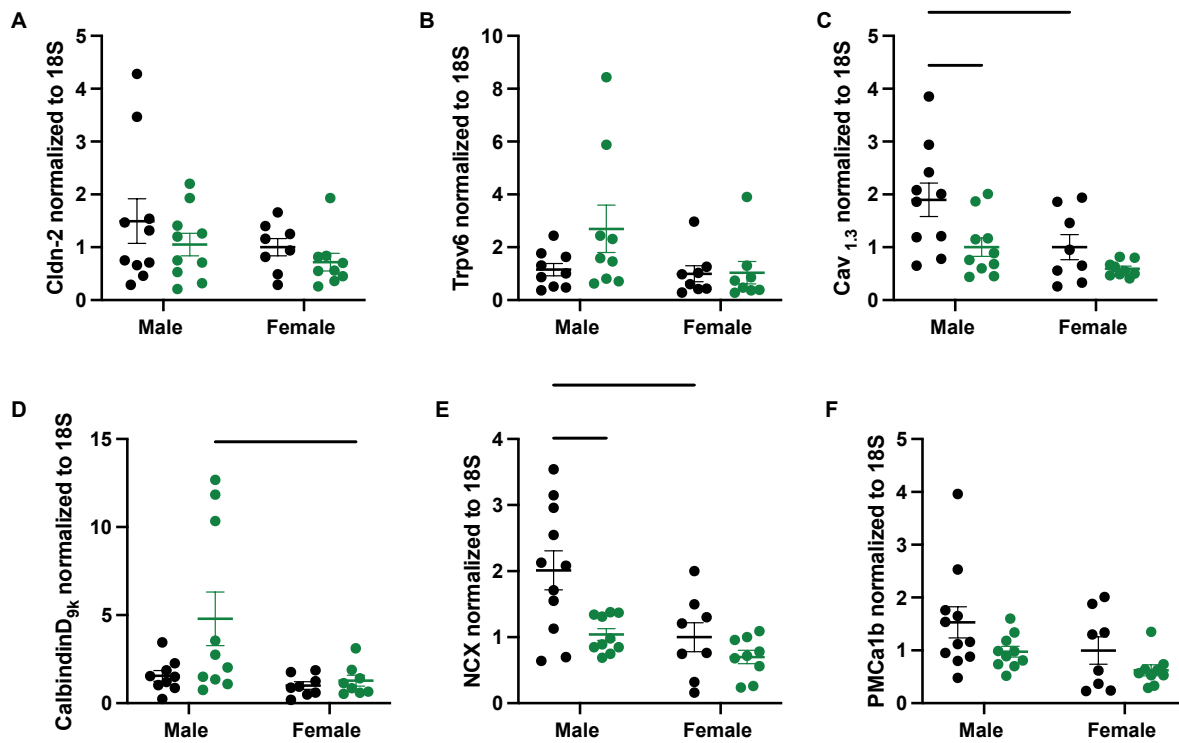


**Figure 3.6: Gene expression in the proximal colon of *TRPV6*<sup>D541A/D541A</sup> mice.** mRNA abundance of (A) *Cldn2*, (B) *Trpv6*, (C) *Cav1.3*, (D) *Calb9k*, (E) *NCX*, (F) *PMCa1b*. Results are normalized to 18S mRNA abundance. Data is presented as mean ± SEM compared with a 2-way ANOVA, Tukey's multiple comparison. Black dots represent WT animals and green dots are representative of *TRPV6*<sup>D541A/D541A</sup> Mice.

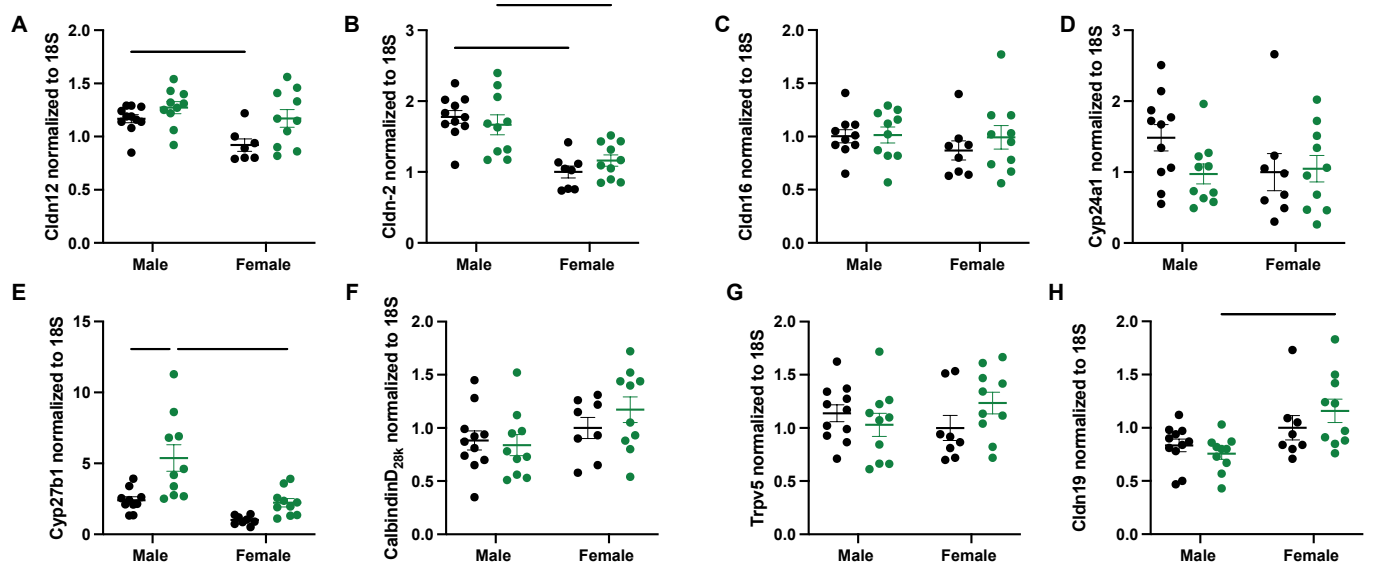


**Figure 3.7: Kidney expression of calcium absorbing pathway genes in *TRPV6<sup>D541A/D541A</sup>***

**mice.** mRNA abundance of (A) *Cldn12*, (B) *Cldn2*, (C) *Cldn16*, (D) *Cyp24a1*, (E) *Cyp27b1*, (F)

*Calb28k*, (G) *Trpv5*, (H) *Cldn19*. Results are normalized to 18S mRNA abundance. Data is

presented as mean  $\pm$  SEM compared with a 2-way ANOVA, Tukey's multiple comparison.

Black dots represent WT animals and green dots are representative of *TRPV6<sup>D541A/D541A</sup>* Mice.

## CLDN2-TRPV6 DKO ANIMALS HAVE REDUCED BODY WEIGHT, HYPOCALCEMIA AND HYPERCALCURIA

Previously, it was reported that *Cldn2* KO animals experience hypercalciuria but no changes in blood calcium or changes in compensatory calciotropic hormones.<sup>(46)</sup> Furthermore, work from other groups found that *TRPV6*<sup>D541A/D541A</sup> mice had no significant calcium phenotype on a normal calcium diet whereas on a low calcium diet they were unable to increase intestinal calcium absorption as much as their WT littermates.<sup>(99)</sup> This lack of a significant calcium phenotype was thought to occur due to the compensation of the paracellular pathway by the transcellular pathway and vice versa. To test this hypothesis, metabolic cage studies were performed with *Cldn2-Trpv6* DKO Mice. In doing so, we observed that the dko male animals had a significant reduction in body weight when compared to their WT littermates (Figure 3.8A), however their chow consumption was comparable to that of the WT animals (Figure 3.8B). Female mice had a lower body weight when compared to male animals (Figure 3.8A). Female WT animals also had an overall significant increase in water consumption for a 24-hour period when compared to the WT male animals (Figure 3.8C). DKO male animals had a significant increase in chow consumption when normalized to their lower body weight (Figure 3D). The dko animals regardless of sex showed similar excreted urine volume to their WT littermates (Figure 3.8E). Female WT animals when compared to male WT animals has a higher mass of feces excreted, presumably because they also have a higher chow consumption, however no differences were observed when comparing dko and WT mice (Figure 3.8F).

A significant reduction in ionized blood calcium (iCa) was seen in both the male and female dko animals when compared to their WT littermates (Figure 3.9A). Due to homeostatic changes in response to lower iCa<sup>2+</sup>, blood PTH levels and calcitriol levels were expected to

increase significantly. Male dko animals showed a significant increase in PTH whereas there was a trend to increased PTH in females, but these differences were not significant (Figure 3.9B). However, blood calcitriol levels were significantly increased in both male and female dko animals as expected (Figure 3.9C).

Additionally, we measured the calcium over creatinine ratio in the dko animals and found that male dko animals had a 4-fold increase when compared to the male WT animals. The dko males also experienced a significant calcium loss when compared to the TRPV6<sup>D541A/D541A</sup> and claudin 2 KO animals (Figure 3.9D). There is a clear trend to greater renal calcium excretion as the paracellular and transcellular pathways are eliminated. Female dko mice also had a significant increase in their urinary calcium loss when compared to the WT females. This was also true when the dko female mice were compared TRPV6<sup>D541A/D541A</sup> and claudin 2 KO female animals (Figure 3.9D). The urinary phosphate to creatinine ratio was significantly increased in the dko males however this difference was not seen in the female dko animals when compared to the WT females (Figure 3.9E). We measured calcium in the feces as a percentage of food consumed and found that there were no significant differences, indicating that intestinal calcium absorption is unaltered in the dko mice regardless of the sex (Figure 3.9F). Overall, these results provide evidence for net urinary loss of calcium but unaltered intestinal calcium absorption.

Detailed analysis of urine electrolyte excretion normalized to creatine revealed that the dko animals regardless of sex have a significant increase in overall ion excretion in their urine, indicating defective renal reabsorption pathways. Table 3.4 summarizes the ratio of the various ions in the urine to creatinine clearance. Creatinine clearance was not significantly different when WT and dko animals were compared regardless of sex. Male dko animals experience a

significant increase in their urinary  $\text{Mg}^{2+}$ ,  $\text{Na}^+$ ,  $\text{Cl}^-$ ,  $\text{Ca}^{2+}$ , and  $\text{PO}_4^{3-}$ . Female dko mice show a sharp increase in  $\text{Mg}^{2+}$ ,  $\text{Na}^+$  and  $\text{Cl}^-$ . Along with urinary phosphate loss, male dko animals also show a significant increase in phosphate loss through the feces, which indicates altered intestinal phosphate absorption (Table 3.6). Chloride loss is also significantly increased in the dko male animals. No such differences were noted in the fecal ion concentrations of the female mutant animals (Table 3.6).



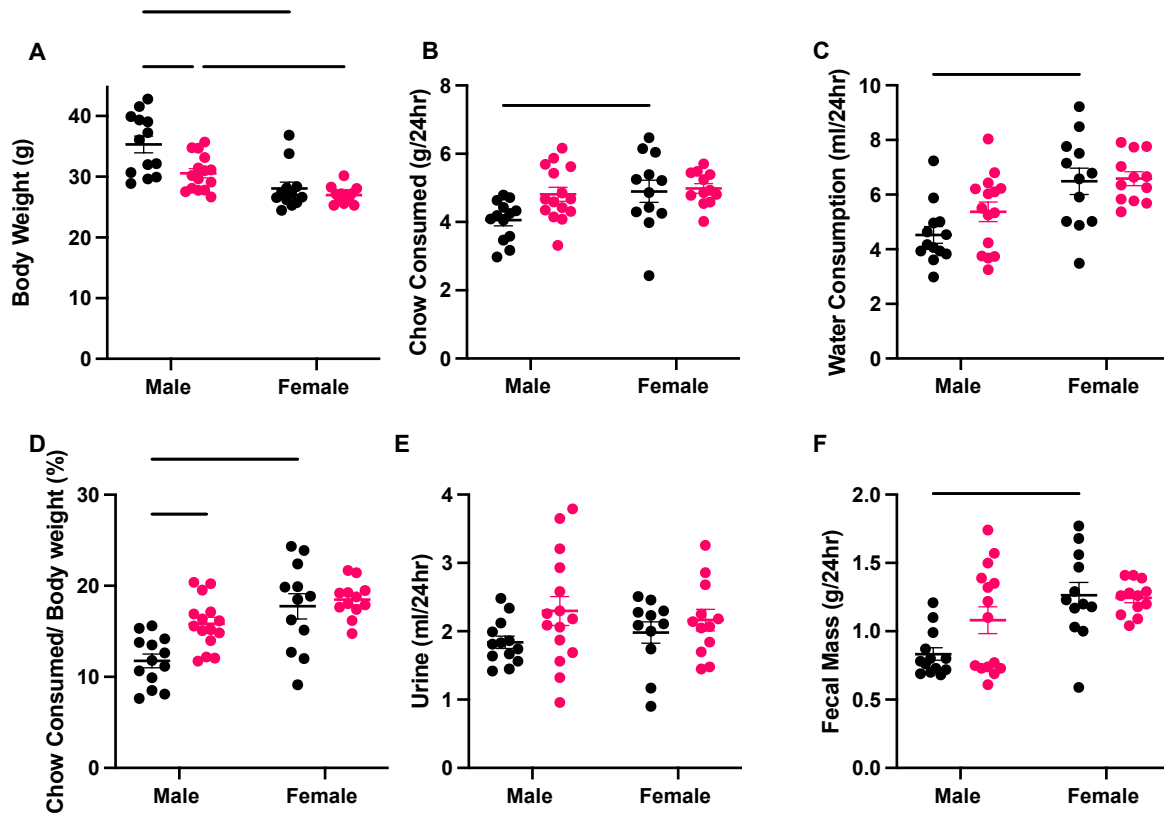


**Figure 3.8: Summary of Metabolic Cage data of  $Cldn2^{-/-}/TRPV6^{D541A/D541A}$  DKO Mice on a Normal Calcium Diet.** (A) Body weight. (B) Chow consumption. (C) Water consumption. (D) Chow consumed as a percentage of body weight. (E) Urine volume voided. (F) Fecal mass excreted in 24 hours.  $n=13$  male WT,  $n=15$  male dko,  $n=12$  female WT,  $n=12$  female dko. All data is presented as mean  $\pm$  SEM compared with a 2-way ANOVA, Tukey's multiple comparison test. Black dots represent WT animals and pink dots are representative of  $Cldn2^{-/-}/TRPV6^{D541A/D541A}$  DKO Mice.

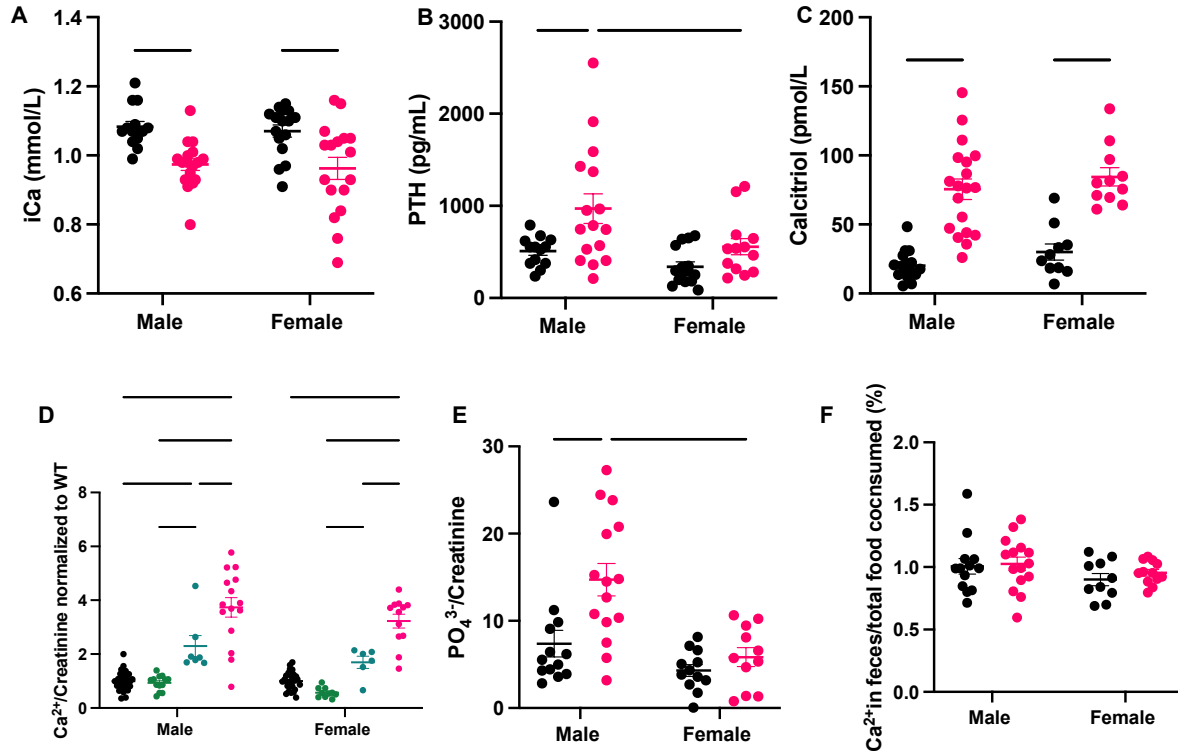


**Figure 3.9: Cldn2-Trpv6 DKO mice have Hypocalcemia, Elevated PTH and Calcitriol levels and Hypercalciuria.** (A) Serum ionized  $\text{Ca}^{2+}$ ,  $n=14$  male WT,  $n=17$  male dko,  $n=16$  female WT,  $n=17$  female dko. (B) Serum PTH levels,  $n=13$  male WT,  $n=16$  male dko,  $n=15$  female WT,  $n=13$  female dko. (C) Serum calcitriol levels,  $n=16$  male WT,  $n=19$  male dko,  $n=10$  female WT,  $n=11$  female KO. (D) Urinary calcium over creatinine ratio normalized to WT animals. (E) Urinary phosphate excretions presented as a ratio of creatinine clearance,  $n=13$  male WT,  $n=15$  male dko,  $n=12$  female WT,  $n=11$  female dko. (F) Fecal calcium excretions as a percentage of total food consumed,  $n=13$  male WT,  $n=15$  male dko,  $n=10$  female WT,  $n=12$  female dko. All data is presented as mean  $\pm$  SEM compared with a 2-way ANOVA, Tukey's multiple comparison test. Black dots represent WT animals, pink dots represent cldn2-trpv6 dko animals, green dots represent  $\text{Trpv6}^{\text{D541A/D541A}}$  mice and lastly blue dots are representative of cldn2 ko animals.

Urine Ion/ Creatinine	Male			Female		
	WT	DKO	p-value	WT (Female)	DKO (Female)	p-value
<b>Ca<sup>2+</sup></b>	0.52 ± 0.05	1.93 ± 0.19	<b>&lt;0.0001</b>	1.10 ± 0.13	3.56 ± 0.28	<b>&lt;0.0001</b>
<b>Mg<sup>2+</sup></b>	3.32 ± 0.76	7.01 ± 0.86	<b>&lt;0.0001</b>	6.26 ± 0.24	3.42 ± 0.91	<b>0.023</b>
<b>K<sup>+</sup></b>	116 ± 6.93	129 ± 4.45	0.265	132 ± 5.43	139 ± 4.28	0.792
<b>Na<sup>+</sup></b>	55.2 ± 2.86	63.6 ± 2.30	<b>0.012</b>	48.2 ± 3.07	60.0 ± 2.71	<b>0.016</b>
<b>Cl<sup>-</sup></b>	123 ± 7.02	142 ± 5.11	<b>0.009</b>	134 ± 6.24	156 ± 4.82	<b>0.038</b>
<b>PO<sub>4</sub><sup>3-</sup></b>	7.39 ± 1.53	14.7 ± 1.86	<b>0.003</b>	4.31 ± 0.67	5.85 ± 1.08	0.894

**Table 3.4: Cldn2-Trpv6 dko mice urine ion normalized to urine creatinine.** Data is presented as mean ± SEM. The results were compared using a 2-way ANOVA, Tukey's multiple comparison test.

	Male			Female		
24-hour Ion (mg)	WT	DKO	p-value	WT	DKO	p-value
<b>Ca<sup>2+</sup></b>	0.12 ± 0.01	0.69 ± 0.10	<b><i>0.0002</i></b>	0.37 ± 0.05	1.28 ± 0.14	<b><i>&lt;0.0001</i></b>
<b>Mg<sup>2+</sup></b>	0.47 ± 0.12	1.52 ± 0.24	<b><i>0.0007</i></b>	1.24 ± 0.10	0.72 ± 0.20	0.228
<b>K<sup>+</sup></b>	26 ± 1	42 ± 4	<b><i>0.003</i></b>	42.9 ± 3.66	47.3 ± 2.90	0.654
<b>Na<sup>+</sup></b>	7.40 ± 0.38	12.0 ± 0.87	<b><i>0.0002</i></b>	9.24 ± 0.86	11.8 ± 0.60	0.096
<b>Cl<sup>-</sup></b>	25.0 ± 1.01	41.7 ± 3.51	<b><i>0.0009</i></b>	39.8 ± 3.61	48.0 ± 2.79	0.253
<b>PO<sub>4</sub><sup>3-</sup></b>	4.08 ± 0.68	10.88 ± 1.12	<b><i>&lt;0.0001</i></b>	3.19 ± 0.51	5.35 ± 1.06	0.384
<b>Creatinine (mM)</b>	3.33 ± 0.25	3.92 ± 0.42	0.835	5.41 ± 0.82	4.30 ± 0.43	0.456

**Table 3.5: Cldn2-Trpv6 dko mice 24-hour urine biochemistry.** Data is presented as mean ± SEM. The results were compared using a 2-way ANOVA, Tukey's multiple comparison test.

	Male			Female		
	WT	DKO	p-value	WT	DKO	p-value
<b>Ca<sup>2+</sup></b>	1.01 ± 0.06	1.03 ± 0.05	0.992	0.900 ± 0.05	0.954 ± 0.03	0.904
<b>Mg<sup>2+</sup></b>	0.141 ± 0.01	0.157 ± 0.01	0.348	0.139 ± 0.005	0.147 ± 0.003	0.860
<b>K<sup>+</sup></b>	0.114 ± 0.01	0.224 ± 0.02	<b>&lt;0.0001</b>	0.162 ± 0.01	0.190 ± 0.02	0.592
<b>Na<sup>+</sup></b>	0.07 ± 0.01	0.08 ± 0.01	0.889	0.108 ± 0.01	0.084 ± 0.01	0.052
<b>Cl<sup>-</sup></b>	13.6 ± 0.77	18.0 ± 1.05	<b>0.0007</b>	15.7 ± 0.36	15.8 ± 0.31	0.999
<b>PO<sub>4</sub><sup>3-</sup></b>	1.19 ± 0.08	1.28 ± 0.07	0.716	1.20 ± 0.05	1.17 ± 0.03	0.984

**Table 3.6: Cldn2-Trpv6 dko mice 24-hour ion excretions in feces normalized to food intake, presented as a percentage.** Data is presented as mean ± SEM. The results were compared using a 2-way ANOVA, Tukey's multiple comparison test.

## CLDN2-TRPV6 DKO MICE SHOW ALTERED BONE MICROARCHITECTURE

Next, we sought to determine if compensatory changes were taking place in the bones of the dko animals. An increase in circulating PTH would target the bones and increase bone resorption to correct for decreased intestinal calcium absorption. Previous work with *Cldn2* KO mice has shown that trabecular bone mineral density is unaffected by a claudin 2 deletion<sup>(46)</sup>, similarly, *TRPV6*<sup>D541A/D541A</sup> mice at six months of age had no changes in bone microarchitecture or bone mineral density.<sup>(111)</sup> We analyzed trabecular bones of *Cldn2*<sup>-/-</sup>/*Trpv6*<sup>D541A/D541A</sup> animals at 18 weeks of age using micro-CT and found that trabecular bone mineral density was not significantly reduced in either male or female dko animals (Figure 3.10A). We did observe alterations to bone microarchitecture, as the percent trabecular bone volume was significantly reduced in male dko animals (Figure 3.10B). Furthermore, trabecular thickness was unaltered in male animals, however there was a significant decrease in female dko animals (Figure 3.10C). Female dko animals had a significant decrease in trabecular thickness when compared to WT female animals (Figure 3.10C). We also noted a sharp increase in trabecular separation which indicates fewer trabecular projections in the dko male animals (Figure 3.10D). Cortical tissue mineral density and percent bone volume were significantly reduced in male dko animals; however, a significant decrease in female dko animals was not detected (Figure 3.10F). In general, female mutant animals had significantly higher cortical TMD and cortical bone volume (Figure 3.10E&F).

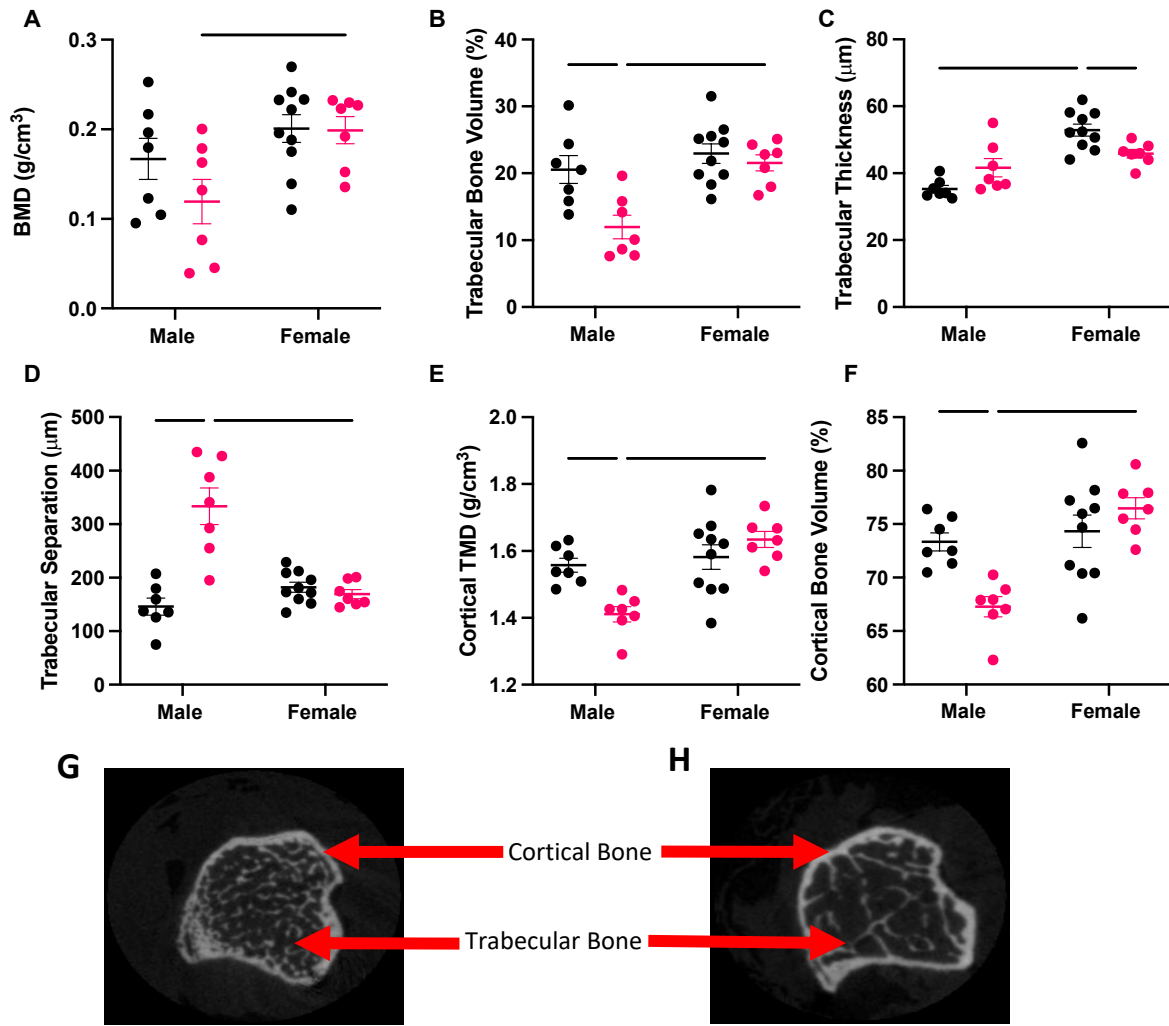


**Figure 3.10: Cldn2-Trpv6 dko animals altered bone microarchitecture and male animals have reduced cortical bone mineral density.** Tibial bone parameters of mice at 18 weeks of age. (A) Trabecular bone mineral density. (B) Percent trabecular bone volume. (C) Trabecular thickness. (D) Trabecular separation. (E) Cortical tissue mineral density. (F) Percent cortical bone volume. (G) WT Male Trabecular Bone Scan. (F) Cldn2-Trpv6 dko Bone Scan. n= 7 male WT, n= 7 male dko, n=10 female WT, n=7 female dko. All data is presented as mean ± SEM compared with a 2-way ANOVA, Tukey's multiple comparison test. Black dots represent WT animals and pink dots are representative of Cldn2<sup>-/-</sup>/TRPV6<sup>D541A/D541A</sup> DKO Mice.

## CLDN2-TRPV6 DKO MICE DEMONSTRATE INTESTINAL AND RENAL COMPENSATION, HOWEVER THIS APPEARS TO BE INADEQUATE

Next, we measured the expression of intestinal calcium absorption genes to evaluate for compensatory increases in alternative pathways to those deleted in the model. We confirmed the deletion of claudin-2 in both male and female dko animals as its expression was not detectable in the duodenum, jejunum, ileum, and proximal colon (Figure 3.11-14 panel A). We noted no significant changes in the mRNA abundance of *Trpv6* in the duodenum, jejunum, or ileum (Figure 3.11-14 panel B) in either sex. *Cav1.3* expression was higher in both WT and dko female animals in the jejunum when compared to the male animals (Figure 3.12C). Female dko animals had a significant increase in the expression of *Pmca1b* in the duodenum when compared to their WT littermates, (Figure 3.11F). However, no alteration in the expression of *Pmca1b* was detected in the male animals in any of the tissue segments assayed (Figure 3.11-14 panel F). *Calb9k* expression was significantly decreased in the dko male animals, presumably due to decreased calcium influx by the non-functional *Trpv6* channel (Figure 3.11D).

Claudin-12 expression, another tight junction protein responsible for forming cation permeable pores, was not significantly altered in the proximal colon in either of the sexes (Figure 3.14B).<sup>(45)</sup> Claudin-15 expression was not significantly altered in either male or female dko animals when compared to their WT littermates (Figure 3.14C). This tight junction protein has also been implicated in cation pore formation.<sup>(44,128)</sup> *Trpv6* expression was significantly increased in the male dko mice, however this would not increase intestinal calcium absorption as the channel has been mutated to be non-functional in these mice. The increase in *Trpv6* can be explained by the increased calcitriol levels which act on *Trpv6* channels to increase intestinal calcium absorption.<sup>(129)</sup> The difference in *Trpv6* expression, although increased was not



significantly so in the female dko animals when compared to their WT littermates (Figure 3.14D). Next, we looked at the expression of *Cacna1d*, which encodes for Cav1.3, an apical L type calcium channel and we found that expression was not altered in the dko animals regardless of sex (Figure 3.14E).<sup>(54)</sup> We observed a significant increase in S100g expression, a gene encoding for the calcium binding protein calbindin-D<sub>9k</sub>, in both the male and female animals (Figure 3.14F). We also observed that female dko animals had an even higher expression of calb9k when they were compared to the dko males (Figure 3.14F). Slc8A1 encoding for *NCX1* and Atp2b1 which encodes for *PMCa1b* both were unaltered in the dko animals in the two sexes (Figure 3.14G&H). Taken together these results indicate an increase in transcellular calcium absorption, indicated by the increase in intracellular calcium concentration as evidenced by the increase in calb9k gene expression which could be calcitriol dependent.

To further understand the compensation that may be occurring in the kidneys we looked at the expression of various genes that are responsible for calcium reabsorption along the nephron. The majority of the filtered calcium is reabsorbed in proximal tubule by claudin 2 and clcn12.<sup>(46,74)</sup> Again, the non-existent gene expression of claudin 2 in the kidneys of the dko animals confirms that the gene encoding claudin 2 was indeed deleted (Figure 3.15A). However, we saw no changes in claudin 12 gene expression in the dko mice regardless of sex (Figure 3.15B). Claudins 16 and 19 are expressed in the thick ascending limb and are responsible for forming divalent cation permeable pores.<sup>(74,75,130)</sup> In our genetically modified dko model we observed increased expression of claudin 16 in the dko males, but the difference was not significant in female dko mice (Figure 3.15C). We observed no change in claudin 19 expression in the male dko mice, females had significantly reduced expression of claudin 19 in the kidney (Figure 3.15D). Furthermore, *Trpv5* mRNA was significantly increased in both female and male

dko animals. The female animals appear to be increasing gene expression even more than the male animals overall (Figure 3.15E). *Trpv5* has been implicated in transcellular calcium reabsorption from the DCT and CNT and contributes to overall fine tuning of calcium levels in the blood.<sup>(8,74,131)</sup> The compensatory increase in transcellular reabsorption in this segment is further supported by a significant increase in *calb28k* (encoded by *Calb1*) gene expression in both the male and female dko mice. Again, the female dko animals appear to be increasing transcellular calcium reabsorption further when compared to the male dko animals (Figure 3.15F). However, the expression of one of the basolateral transporters of calcium, *PMCa1b*, was not significantly altered in either sex (Figure 3.15G) whereas the expression of the other major calcium transporter, *NCX1*, was significantly increased in the female dko mice (Figure 3.15B). Finally, *Cyp27b1*, the main enzyme responsible for regulating the last step in calcitriol activation was significantly upregulated in both the male and female dko animals (Figure 3.14H). *Cyp24a1*, which encodes for 24-hydroxylase, an enzyme responsible for the deactivation of calcitriol was not significantly altered in either sex (Figure 3.15A). Claudin 14, which serves to block the cation permeable pore formed by claudin 16 and claudin 19 in the TAL, showed overall higher expression in the female animals when compared to the male animals (Figure 3.15C). Overall, these results indicate that renal compensation is taking place in the dko animals however this is insufficient to correct for the significant hypocalcemia observed or to even reduce urinary calcium excretion to that of wild-type mice.

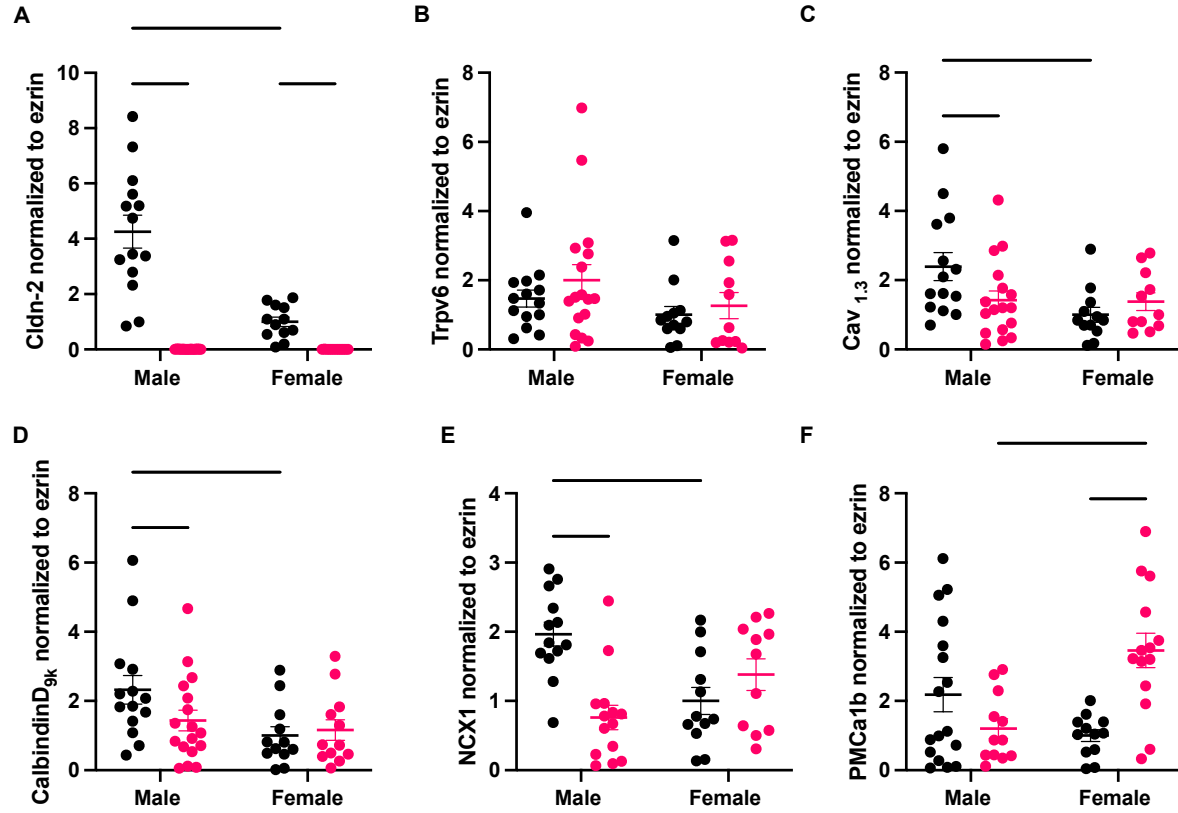


**Figure 3.11: Cldn2-Trpv6 DKO mice mRNA expression of the calcium absorption pathway genes in the duodenum.** mRNA abundance of (A) *Cldn2*, (B) *Trpv6*, (C) *Cav1.3*, (D) *Calb9k*, (E) *NCX1*, (F) *PMCa1b*. Results are normalized to ezrin mRNA abundance. N = 14 male WT, n= 17 male dko, n=12 female WT, n=12 female dko. All data is presented as mean  $\pm$  SEM compared with a 2-way ANOVA, Tukey's multiple comparison test. Black dots represent WT animals and pink dots are representative of *Cldn2*<sup>-/-</sup>/*TRPV6*<sup>D541A/D541A</sup> DKO Mice.

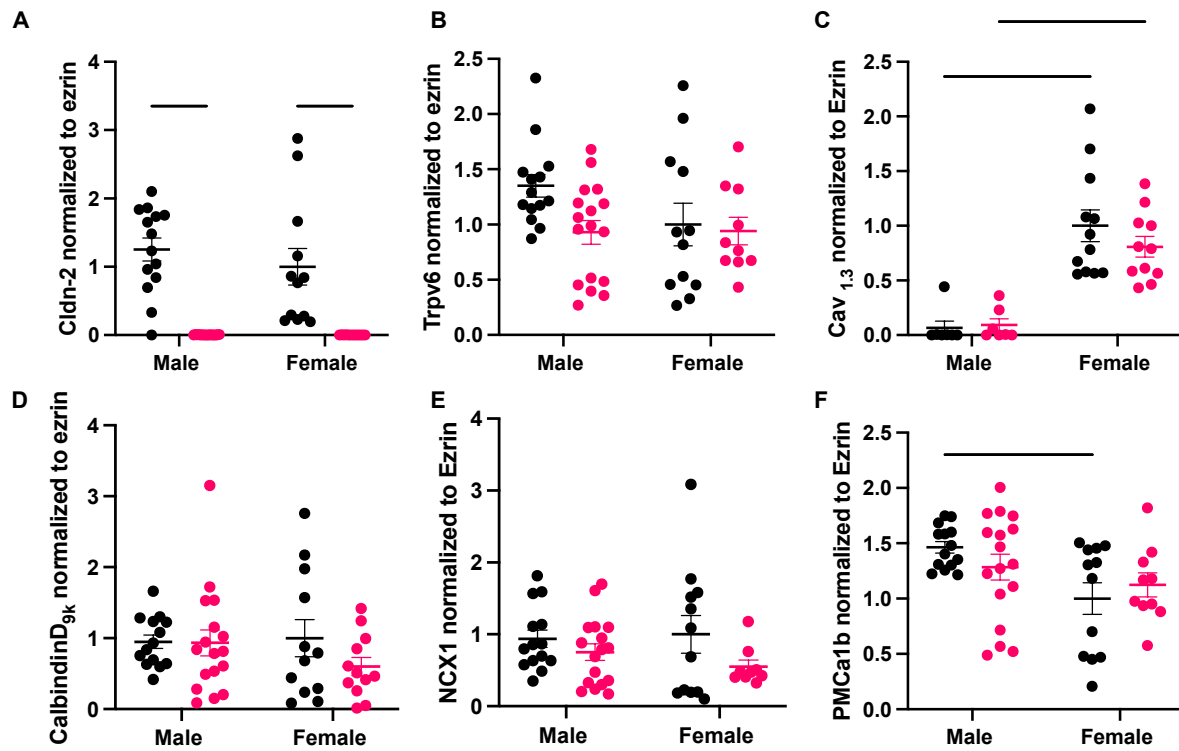


**Figure 3.12: Cldn2-Trpv6 DKO mice mRNA expression of the calcium absorption pathway genes in the jejunum.** mRNA abundance of (A) *Cldn2*, (B) *Trpv6*, (C) *Cav1.3*, (D) *Calb9k*, (E) *NCX1*, (F) *PMCa1b*. Results are normalized to ezrin mRNA abundance. N = 14 male WT, n= 17 male dko, n=12 female WT, n=12 female dko. All data is presented as mean  $\pm$  SEM compared with a 2-way ANOVA, Tukey's multiple comparison test. Black dots represent WT animals and pink dots are representative of *Cldn2*<sup>-/-</sup>/*TRPV6*<sup>D541A/D541A</sup> DKO Mice.

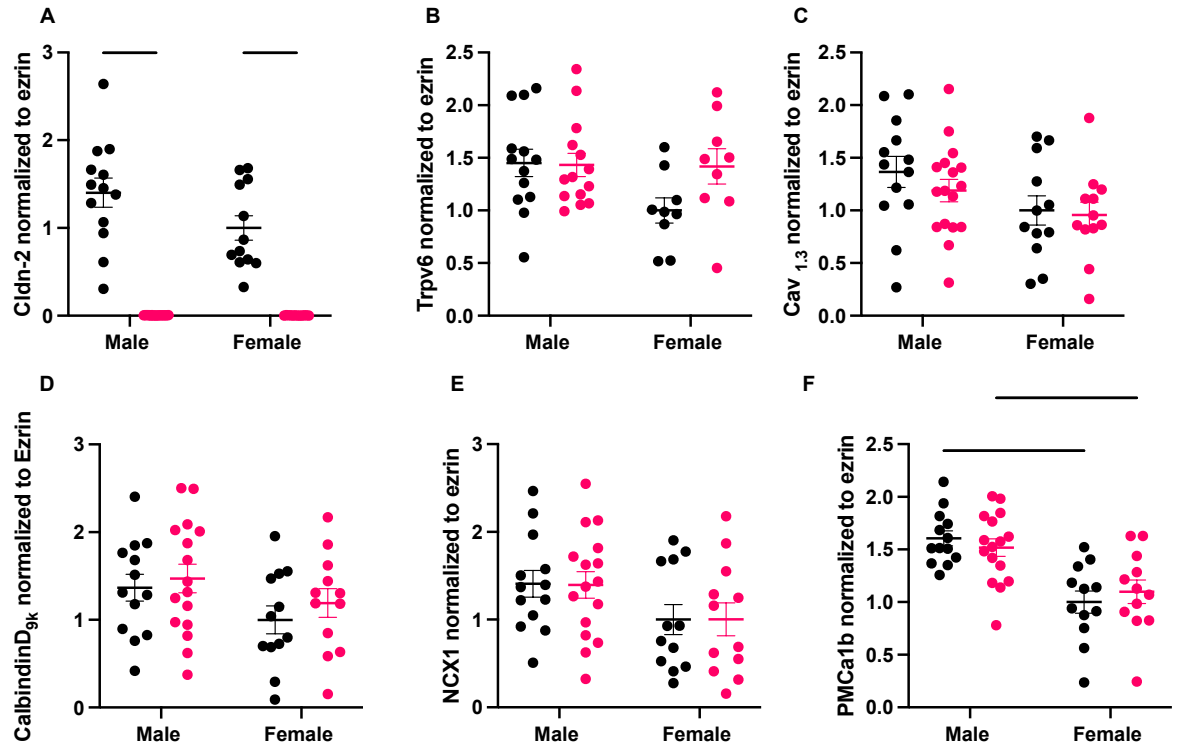


**Figure 3.13: Cldn2-Trpv6 DKO mice mRNA expression of the calcium absorption pathway genes in the ileum.** mRNA abundance of (A) *Cldn2*, (B) *Trpv6*, (C) *Cav1.3*, (D) *Calb9k*, (E) *NCX1*, (F) *PMCa1b*. Results are normalized to ezrin mRNA abundance. N = 14 male WT, n= 17 male dko, n=12 female WT, n=12 female dko. All data is presented as mean  $\pm$  SEM compared with a 2-way ANOVA, Tukey's multiple comparison test. Black dots represent WT animals and pink dots are representative of *Cldn2*<sup>-/-</sup>/*TRPV6*<sup>D541A/D541A</sup> DKO Mice.

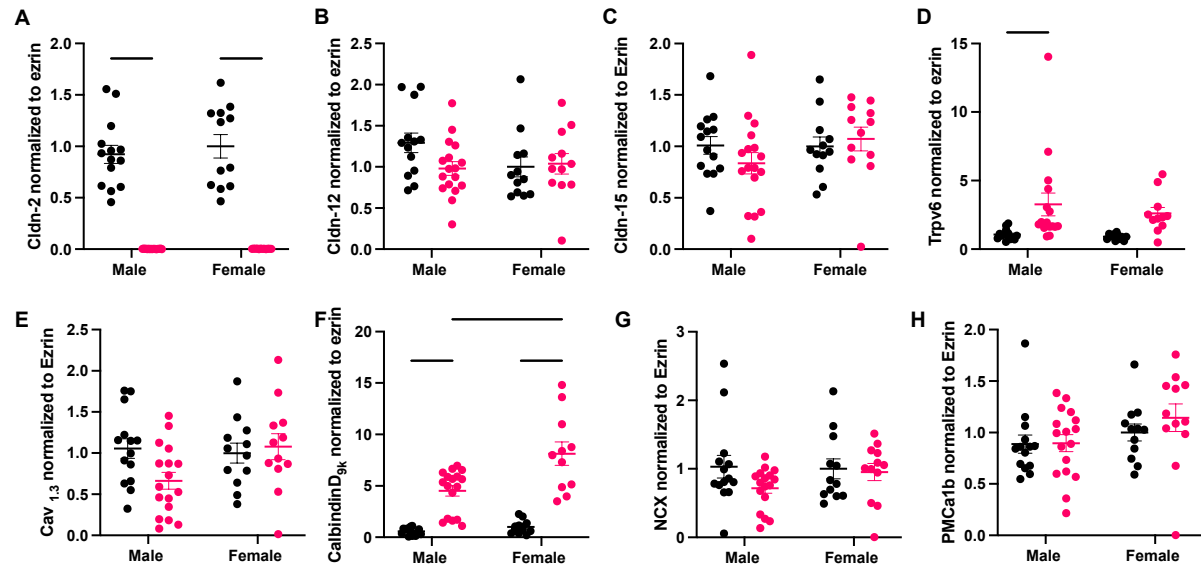


**Figure 3.14: Cldn2-Trpv6 dko animals have compensatory increased calbindinD<sub>9k</sub> expression in the proximal colon.** mRNA abundance of (A) *Cldn2*, (B) *Cldn12*, (C) *Cldn15*, (D) *Trpv6*, (E) *Cav1.3*, (F) *Calb9k*, (G) *NCX*, (H) *PMCa1b*. Results are normalized to ezrin mRNA abundance. 14 male WT, n= 17 male dko, n=12 female WT, n=12 female dko. All data is presented as mean ± SEM compared with a 2-way ANOVA, Tukey's multiple comparison test. Black dots represent WT animals and pink dots are representative of *Cldn2*<sup>-/-</sup>/*TRPV6*<sup>D541A/D541A</sup> DKO Mice.

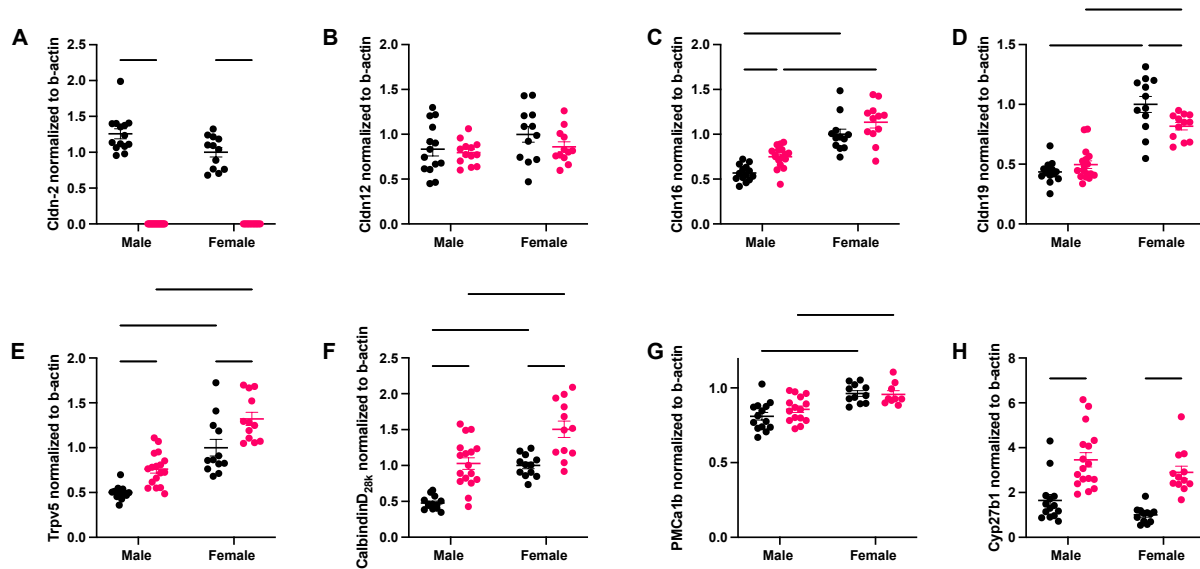


**Figure 3.15: *Cldn2-Trpv6* dko animals display renal compensation.** mRNA abundance of (A) *cldn2*, (B) *cldn12*, (C) *cldn16*, (D) *cldn19*, (E) *Trpv5*, (F) *Calb28k*, (G) *PMCa1b*, (H) *Cyp27b1*, n= 14 male WT, n= 17 male dko, n=12 female WT, n=12 female dko. mRNA abundance has been normalized to beta-actin. All data is presented as mean  $\pm$  SEM compared with a 2-way ANOVA, Tukey's multiple comparison. Black dots represent WT animals and pink dots are representative of *Cldn2*<sup>-/-</sup>/*TRPV6*<sup>D541A/D541A</sup> DKO Mice.

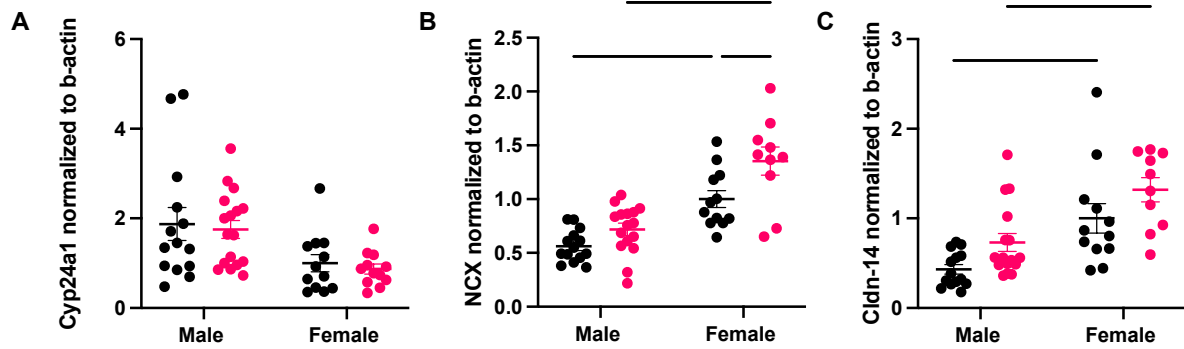


**Figure 3.16: Kidney gene expression of Cldn2-Trpv6 dko mice.** mRNA abundance of (A) *Cyp24a1*, (B) *NCX*, (C) *Cldn14*. Results are normalized to beta actin mRNA abundance. Data is presented as mean  $\pm$  SEM compared with a 2-way ANOVA, Tukey's multiple comparison. Black dots represent WT animals and pink dots are representative of *Cldn2*<sup>-/-</sup>/*TRPV6*<sup>D541A/D541A</sup> DKO Mice.



## **CHAPTER 4: DISCUSSION**

This project aimed to shed light on sex specific differences in the TRPV6<sup>D541A/D541A</sup> mutant mouse model and to delineate the calcium phenotype of a Cldn2-Trpv6 dko mouse model. This latter model system has a deletion of one of the main paracellular pathways mediating calcium absorption from the intestine and a non-functional calcium channel responsible for transcellular intestinal absorption. Consistent with previous work TRPV6<sup>D541A/D541A</sup> mice on a normal calcium diet did not demonstrate a dramatic calcium phenotype. However, we did observe that male mice had mild hypocalcaemia and proportionately increased plasma calcitriol levels, which was not previously reported.<sup>(99)</sup> Further, our lab previously reported that claudin 2 KO animals are hypercalciuric but have normal blood calcium levels and no changes in BMD.<sup>(46)</sup> Based on these observations, we posited that this is due to the paracellular pathway (which is in part composed of claudin-2) is able to compensate for the loss of transcellular calcium absorption in the TRPV6<sup>D541A/D541A</sup> mice and vice versa. We were able to provide some evidence in support of this by generating a double knockout mouse. The dko mice had a worsening calcium phenotype with the dko animals experiencing significant hypocalcaemia and greater hypercalciuria (relative to the claudin-2 KO mice) regardless of sex. However, they did not have altered net intestinal calcium absorption but instead displayed altered bone microarchitecture. Reduced small intestinal calcium absorption appeared to be compensated by the colon as we observed a significant increase in calb9k expression in the proximal colon of the dko mice, consistent with compensatory increased transcellular calcium absorption via a channel other than Trpv6. Along with the compensatory increase in the proximal colon, the dko mice show evidence of compensation in the kidney, however this was not sufficient to normalize plasma calcium nor even lower urinary calcium excretion. In fact, the dko mice had increased urinary calcium excretion beyond even the claudin 2 single knockout

animals. Thus, it appears that the lower plasma calcium in the dko mice is secondary to renal calcium wasting and a failure to sufficiently increase intestinal calcium absorption to compensate.

## ESTROGEN ACTS AS A PROTECTIVE MEASURE IN TRPV6<sup>D541A/D541A</sup> FEMALE MICE FOR THEIR OVERALL CALCIUM BALANCE

Mild perturbations in the overall calcium balance in the TRPV6<sup>D541A/D541A</sup> mice could be attributed to the fact that on a normal calcium diet, calcium is absorbed predominately through a paracellular pathway and transcellular calcium absorption occurs when dietary calcium availability is limited.<sup>(57,105)</sup> As our metabolic cage studies were conducted with animals fed a normal calcium diet, transcellular calcium absorption was potentially limited. However, our investigation of the TRPV6<sup>D541A/D541A</sup> mice revealed a sex specific difference in blood calcium, which has not been previously reported.<sup>(99)</sup> What distinguishes our study from the work previous work is that we separated animals by sex, but this was not clearly reported in the previous study. Furthermore, we measured ionized calcium whereas previous work measured total blood calcium, which includes calcium bound to proteins.<sup>(99)</sup> The previous study used a regular calcium diet that contained 1% calcium whereas the one utilized in our studies was slightly lower at 0.81% calcium, a difference which might also contribute to our slightly discrepant results. Importantly most of our results are consistent with many of the findings previously reported. We also found unaltered body mass, similar chow, and water consumption of the mutant animals. Both our studies and previous work on the Trpv6 mutant mice are in contrast to the findings of the Trpv6 KO animals. These mice display significant alopecia and growth retardation in contrast

to the Trpv6 mutant mice. Our animal model relies on making the channel non-functional rather than completely deleting it from the genome. Having the channel intact allows for interactions with scaffolding proteins that could potentially have other roles. However, the deletion of Trpv6, results in the loss of these other functions which may potentially lead to the more severe outcome observed in the Trpv6 KO animals, when compared to the mutant mice. Of note, the Trpv6 KO mouse generated by Bianco et. al. also has a partial deletion in the EphB6 gene along with the Trpv6 gene, which could potentially be a confounding variable resulting in the greater calcium perturbations seen in the KO animals. Furthermore, animals in our studies were fed a 0.81% calcium diet, whereas the Trpv6 KO mice reported calcium perturbations when animals were fed a 1% calcium diet.<sup>(105)</sup> Interestingly we observed a significant decrease in urinary calcium excretion in the mutant female animals which is likely a compensatory mechanism enabling the maintenance of plasma calcium. To prevent hypocalcaemia, the females respond by decreasing urinary excretion of calcium, whereas the male animals are unable to do so which results in hypocalcaemia.

Consistent with the sex specific differences we observed, many studies have reported a sex dependent increase in urinary calcium loss. Estrogen is known to play a role in increasing calcium reabsorption in the kidneys. Female rats have been found to have more Trpv5 mRNA and protein expression, along with NCX1 and PMCa1b, indicating an increase in the calcium reabsorption machinery in the DCT/CNT.<sup>(132,133)</sup> Hsu et al. reported the effects of testosterone on renal calcium handling in male mice. Male orchietomized mice had reduced urinary calcium excretion and increased expression of calcium channel proteins in the DCT/CNT. Expression of Trpv5 and calb28k in the DCT/CNT was significantly decreased by supplying these animals with testosterone, which resulted in an increase in urinary calcium excretion.<sup>(133)</sup> To correct the

significant drop in blood calcium levels in male animals, calcitriol levels increased significantly. Calcitriol is also a regulator of phosphate homeostasis. Calcitriol increases the expression of the intestinal sodium phosphate cotransporter Napi2b, which increases intestinal phosphate absorption. This then contributes to increased loss of phosphate in the urine as observed in the male mutant animals.<sup>(26,27)</sup>

## CLDN2-TRPV6 DKO MICE HAVE COMPENSATORY INCREASED COLONIC CALCIUM ABSORPTION

Cldn2-Trpv6 dko animals display a significant calcium phenotype as evidenced by urinary calcium loss and low plasma calcium levels. In response to increase urinary loss of calcium, blood levels of parathyroid hormone and calcitriol increase. The hypercalciuria observed in the dko mice is even greater than the claudin 2 ko mice, and much greater than the Trpv6 mutant mice that have either unaltered or reduced urinary calcium excretion.<sup>(46,99)</sup> Despite the increased expression of renal calcium absorption pathway genes, they are unable to compensate. This data provides evidence that both claudin 2 and TRPV6 play a significant role in intestinal calcium absorption and renal reabsorption.

We expected to see a significant reduction in intestinal calcium absorption, measured by an increase in fecal calcium excretion, but this was not observed. No change in intestinal calcium absorption potentially indicates that another calcium channel protein is compensating. The L type channel, Cav1.3, has been suggested as mediating an alternative calcium absorption pathway.<sup>(55,134)</sup> Calcium absorption through this channel is dependent on glucose transport

through SGLT1. Post eating, high luminal glucose availability results in absorption of glucose and sodium through SGLT1. This creates a local depolarizing environment which facilitates the opening of Cav1.3 and therefore calcium entry into the cell.<sup>(55)</sup> Previous work done with *Cacna1d* KO pups shows a complete loss of transcellular calcium flux across the jejunum, when measured *ex vivo* in Ussing chambers.<sup>(54)</sup> Furthermore, perfusion of rat jejunum also found a significant reduction in calcium absorption in the presence of the L type channel inhibitor, nifedipine.<sup>(55,68,135)</sup> Work with caco-2 monolayers, found that prolactin increases calcium flux across the cell layer, however this increase was prevented by either nifedipine or verapamil, both of which are L type calcium channel blockers. Furthermore, the authors were able to show that caco-2 cells transfected with siRNA, targeting Cav1.3, results in complete abolition of transcellular calcium flux.<sup>(136)</sup> These studies further implicate Cav1.3 as an alternative intestinal calcium absorption pathway. In our experiments we did not note a significant increase in expression of Cav1.3 in any of the intestinal segments of the *cldn2-trpv6* dko mice, however increased flux through this channel is still possible under normal expression conditions. Future experiments should examine calcium flux across the different intestinal segments in Ussing chambers. A significant increase in calcium absorption through Cav1.3 could explain the increased expression of calb9k in the proximal colon. Increased calcium flux into the cell leads to a significant increase in calb9k expression to prevent the toxic effects of free calcium.<sup>(137)</sup>

We observed a significant reduction in blood  $iCa^{2+}$  levels in the dko animals along with a significant increase in calcitriol and PTH and marked renal calcium wasting. PTH has known functions that include increased bone resorption, because of this we expected to see a significant decrease in trabecular bone mineral density in the dko male and female animals. However, this was not the case, but we did observe other alterations in bone microarchitecture. Previous work

with claudin 2 ko animals and P14 Trpv6<sup>D541A/D541A</sup> mice found no significant decrease in bone microarchitecture of adult animals.<sup>(46,54)</sup> In contrast we observed that the male dko animals had a significant decrease in overall cortical tissue mineral density and bone volume. Along with this they displayed increased trabecular separation and trabecular number. This decline in bone health was likely due to the actions of PTH on bone resorption. PTH causes increase bone breakdown to replenish the reduced  $iCa^{2+}$  in the blood.<sup>(13,42)</sup>

## ALTERNATIVE PARACELLULAR CALCIUM ABSORPTION THROUGH CLAUDIN-12

Due to the inactivation of Trpv6 and deletion of Cldn2 in the intestines we expected to observe a significant increase in calcium excretion in the feces of the dko mice due to reduced absorption. However, this was not the case, and thus we sought to identify alternative calcium absorption pathways in the intestinal segments that were compensating. Along with claudin-2, claudin-12 also plays a role in calcium absorption and reabsorption in the renal proximal tubule.<sup>(45,78)</sup> In the dko mice we posit increased calcium absorption through claudin-12, when claudin-2 was deleted. It has been reported that claudin-2 and claudin-12 form independent pores and both are important in maintaining calcium homeostasis.<sup>(29,45,78)</sup> Previous work has shown variable expression of claudin-12 along the intestine with the highest expression in the ileum, moderate expression in the jejunum and colon and very low expression in the duodenum.<sup>(138)</sup> Expression of claudin-12, along with claudin-2 has also been found to be affected by calcitriol. Fujita et al. reported a 75% reduction in claudin-12 expression along the colon and ileum of vitamin D receptor KO animals when compared to WT mice. Normally, treatment of caco2 cells with calcitriol causes a reduction in transepithelial resistance (TER) which increases calcium

permeability.<sup>(29)</sup> However, when claudin-2 and claudin-12 were knocked down in caco2 cells, this effect was significantly attenuated. This is consistent with calcium permeability through claudin-2 and claudin-12 being affected by calcitriol. Over expressing claudin-12 caused an increase in calcium permeability in caco2 cells.<sup>(29)</sup> Of note, we did not observe a significant increase in claudin-12 mRNA in any of the intestinal segments of *cldn2-trpv6* dko mice. However, we did not measure protein levels due to the lack of a specific antibody. This study provides evidence for a role of claudin-12 in intestinal calcium absorption. Studies with *cldn2/12* dko mice provide further evidence of the importance of claudin-12 in calcium absorption as the dko mice have a significant reduction in serum calcium, along with significantly reduced bone mineral density.<sup>(45)</sup> Furthermore, claudin-12 ko mice show reduced paracellular permeability in the proximal tubule.<sup>(78)</sup> Overall, significant paracellular absorption of calcium along the intestines could account for the phenotype observed in the *Cldn2-Trpv6* dko animals. However, further studies need to be done to assess whether claudin-12 plays a protective role in the *Cldn2-Trpv6* dko model by increasing paracellular calcium absorption.

## FUTURE DIRECTIONS

To determine if Cav1.3 and SGLT1 play a role by increasing intestinal calcium absorption in the dko animals in compensation, it is worthwhile to assess the effects of administering a SGLT1 inhibitor to wildtype and dko animals and noting alterations to calcium homeostasis. Because SGLT1 mediates the opening of Cav1.3, assessing the effects that an L type calcium channel blocker has on calcium homeostasis in wildtype and dko mice may shed light into atypical transcellular calcium channel pathways. This could be accomplished by



placing the dko mice in metabolic cages permitting a baseline collection of urine and feces. They could then be fed a diet containing either the SGLT inhibitor (Sotagliflozin) or the L-type calcium channel blocker (Felodipine) and urine and feces collected. A paired analysis of urine and fecal calcium excretion could then be performed. If compensation is occurring through our proposed pathway, we predict that both drugs will significantly reduce intestinal calcium absorption in the dko mice but not the wild-type mice. Furthermore, another series of experiments, using *ex vivo* Ussing chamber studies could be conducted to measure net radioactive calcium flux across intestinal segments of wild-type and dko mice in the presence and absence of the SGLT or a L-type calcium channel blocker. These experiments will be necessary to pinpoint the exact segment of the intestine responsible for compensatory increased calcium absorption. Alternatively, generating a *cldn2/trpv6/cav1.3* triple knockout mouse model could help identify the importance of Cav1.3 in intestinal calcium absorption and renal reabsorption.

To test whether claudin-12 is contributing compensatory paracellular calcium absorption in the dko mice, the Alexander laboratory is generating a *cldn2/cldn12/trpv6* triple ko mouse model. Based on the work done on *cldn2* ko, *cldn12* ko and *cldn2/12* dko mice as well as the *Trpv6* mutant mice and the *Cldn2/Trpv6* dko animals, the triple ko animals are expected to have severe disruptions in calcium homeostasis. We predict that these animals will be severely hypocalcemic due to defective calcium absorption in the intestine and defective renal calcium handling. Due to decreased net calcium balance, these mice are expected to respond by increasing PTH and calcitriol levels, the combined effects of which will cause severe bone resorption, in an attempt to correct for the low blood calcium. It will be interesting to further explore what compensation, if any, occurs in other known calcium transporter such as Cav1.3 in the intestinal segments to correct for decreased intestinal calcium absorption. If Cav1.3 and

SGLT1 expression is increased, this would provide further insight into when these channels are more active i.e., under conditions where other primary calcium absorption pathways are not available. It will also be important to look for renal compensation in the more distal part of the nephron and if there are any unique sex differences that are present.

In summary, our work with Trpv6 mutant mice shows that there is a sex specific difference in calcium absorption, the underlying reason for which is not clear and not previously reported. Furthermore, our novel Cldn2-Trpv6 DKO mice show us the importance of both the paracellular and the transcellular pathway in calcium absorption in mice. Both pathways are necessary to maintain calcium homeostasis and overall health as having defects in both pathways results in hypocalcaemia and significant renal calcium wasting which is unable to be compensated by an increase in the hormones PTH and calcitriol.

## References

1. Peacock M. Calcium metabolism in health and disease. Vol. 5, Clinical Journal of the American Society of Nephrology. 2010.
2. Vannucci L, Fossi C, Quattrini S, Guasti L, Pampaloni B, Gronchi G, et al. Calcium Intake in bone health: A focus on calcium-rich mineral waters. Vol. 10, Nutrients. MDPI AG; 2018.
3. Beggs MR, Bhullar H, Dimke H, Alexander RT. The contribution of regulated colonic calcium absorption to the maintenance of calcium homeostasis. Journal of Steroid Biochemistry and Molecular Biology. 2022 Jun 1;220.
4. Veldurthy V, Wei R, Oz L, Dhawan P, Jeon YH, Christakos S. Vitamin D, calcium homeostasis and aging. Vol. 4, Bone Research. Sichuan University; 2016.
5. Areco VA, Kohan R, Talamoni G, Tolosa De Talamoni NG, Peralta López ME. Intestinal Ca<sup>2+</sup>absorption revisited: A molecular and clinical approach. Vol. 26, World Journal of Gastroenterology. Baishideng Publishing Group Co; 2020. p. 3344–64.
6. Morris HA, Need AG, Horowitz M, O'loughlin PD, Nordin BEC. Calcified Tissue International Calcium Absorption in Normal and Osteoporotic Postmenopausal Women. Vol. 49, Calcif Tissue Int. 1991.
7. Golden NH, Abrams SA, Daniels SR, Corkins MR, De Ferranti SD, Magge SN, et al. Optimizing bone health in children and adolescents. Vol. 134, Pediatrics. American Academy of Pediatrics; 2014. p. e1229–43.
8. Hoenderop JGJ, Nilius B, Bindels RJM. Calcium Absorption Across Epithelia. 2005; Available from: [www.prv.org](http://www.prv.org)
9. Rendina-Ruedy E, Rosen CJ. Parathyroid hormone (PTH) regulation of metabolic homeostasis: An old dog teaches us new tricks. Vol. 60, Molecular Metabolism. Elsevier GmbH; 2022.
10. Potts JT. Parathyroid hormone: Past and present. Vol. 187, Journal of Endocrinology. 2005. p. 311–25.
11. Ritter CS, Haughey BH, Miller B, Brown AJ. Differential gene expression by oxyphil and chief cells of human parathyroid glands. Journal of Clinical Endocrinology and Metabolism. 2012 Aug;97(8).
12. Alexander RT, Dimke H. Effects of parathyroid hormone on renal tubular calcium and phosphate handling. Acta Physiologica. 2023 May 9;
13. Kužma M, Jackuliak P, Killinger Z, Payer J. Parathyroid Hormone-Related Changes of Bone Structure. Physiol Res. 2021;70:3–11.
14. Tominaga N, Yonaha T, Yamanouchi M, Sumi H, Taki Y, Shibagaki Y, et al. Bone responsiveness to parathyroid hormone is negatively associated with parathyroid hormone-lowering drug use in patients undergoing hemodialysis: a cross-sectional study. BMC Nephrol. 2021 Dec 1;22(1).
15. Fan Y, Hanai J ichi, Le PT, Bi R, Maridas D, DeMambro V, et al. Parathyroid Hormone Directs Bone Marrow Mesenchymal Cell Fate. Cell Metab. 2017 Mar 7;25(3):661–72.
16. Young K, Beggs MR, Grimbley C, Alexander RT. Regulation of 1 and 24 hydroxylation of vitamin D metabolites in the proximal tubule. Vol. 247, Experimental Biology and Medicine. SAGE Publications Inc.; 2022. p. 1103–11.

17. Abel M Van, Hoenderop JGJ, Van Der Kemp AWCM, Friedlaender MM, Van Leeuwen JPTM, Ren' R, et al. Coordinated control of renal Ca<sup>2+</sup> transport proteins by parathyroid hormone. Vol. 68, *Kidney International*. 2005.
18. Lee M, Partridge NC. Parathyroid hormone signaling in bone and kidney. Vol. 18, *Current Opinion in Nephrology and Hypertension*. 2009. p. 298–302.
19. Xue Y, Fleet JC. Intestinal Vitamin D Receptor Is Required for Normal Calcium and Bone Metabolism in Mice. *Gastroenterology*. 2009;136(4).
20. Saponaro F, Saba A, Zucchi R. An update on vitamin d metabolism. Vol. 21, *International Journal of Molecular Sciences*. MDPI AG; 2020. p. 1–19.
21. Gil Á, Plaza-Diaz J, Mesa MD. Vitamin D: Classic and Novel Actions. *Ann Nutr Metab*. 2018 Mar 1;72(2):87–95.
22. Fleet JC. Vitamin D-Mediated Regulation of Intestinal Calcium Absorption. Vol. 14, *Nutrients*. MDPI; 2022.
23. Wang Y, Zhu J, Deluca HF, Deluca HF. The vitamin D receptor in the proximal renal tubule is a key regulator of serum 1,25-dihydroxyvitamin D<sub>3</sub>. *Am J Physiol Endocrinol Metab* [Internet]. 2015;308:201–5. Available from: <http://www.ajpendo.org>
24. Fleet JC. The role of vitamin D in the endocrinology controlling calcium homeostasis. Vol. 453, *Molecular and Cellular Endocrinology*. Elsevier Ireland Ltd; 2017. p. 36–45.
25. Diaz De Barboza G, Guizzardi S, Tolosa De Talamoni N. Molecular aspects of intestinal calcium absorption. *World J Gastroenterol*. 2015 Jun 21;21(23):7142–54.
26. Christakos S. Vitamin D: A Critical Regulator of Intestinal Physiology. Vol. 5, *JBMR Plus*. John Wiley and Sons Inc; 2021.
27. Pike JW, Christakos S. Biology and Mechanisms of Action of the Vitamin D Hormone. Vol. 46, *Endocrinology and Metabolism Clinics of North America*. W.B. Saunders; 2017. p. 815–43.
28. Van Cromphaut SJ, Dewerchin M, Hoenderop JGJ, Stockmans I, Herck E Van, Kato S, et al. Duodenal calcium absorption in vitamin D receptor-knockout mice: Functional and molecular aspects. *PNAS* [Internet]. 2001;98(23). Available from: [www.pnas.org](http://www.pnas.org)
29. Fujita H, Sugimoto K, Inatomi S, Maeda T, Osanai M, Uchiyama Y, et al. Tight Junction Proteins Claudin-2 and-12 Are Critical for Vitamin D-dependent Ca<sup>2+</sup> Absorption between Enterocytes. *Mol Biol Cell* [Internet]. 2008;19:1912–21. Available from: <http://www.molbiolcell.org/cgi/doi/10.1091/mbc.E07-09>
30. Hoenderop JGJ, Van Der Kemp AWCM, Urben CM, Strugnell SA, Bindels RJM. Effects of vitamin D compounds on renal and intestinal Ca<sup>2+</sup> transport proteins in 25-hydroxyvitamin D<sub>3</sub>-1 $\alpha$ -hydroxylase knockout mice. *Kidney Int*. 2004;66(3):1082–9.
31. Murali SK, Roschger P, Zeitz U, Klaushofer K, Andrukhova O, Erben RG. FGF23 Regulates Bone Mineralization in a 1,25(OH)<sub>2</sub>D<sub>3</sub> and Klotho-Independent Manner. *Journal of Bone and Mineral Research*. 2016 Jan 1;31(1):129–42.
32. Miedlich SU, Zhu ED, Sabbagh Y, Demay MB. The receptor-dependent actions of 1,25-dihydroxyvitamin D are required for normal growth plate maturation in Npt2a knockout mice. *Endocrinology*. 2010;151(10):4607–12.
33. Nakamichi Y, Udagawa N, Suda T, Takahashi N. Mechanisms involved in bone resorption regulated by vitamin D. Vol. 177, *Journal of Steroid Biochemistry and Molecular Biology*. Elsevier Ltd; 2018. p. 70–6.
34. Felsenfeld AJ, Levine BS. Calcitonin, the forgotten hormone: Does it deserve to be forgotten? *Clin Kidney J*. 2015 Apr 1;8(2):180–7.

35. Srinivasan A, Wong FK, Karponis D. Calcitonin: A useful old friend [Internet]. 2020. Available from: <http://www.ismni.org>
36. Matikainen N, Pekkarinen T, Ryhänen EM, Schalin-Jäntti C. Physiology of Calcium Homeostasis: An Overview. Vol. 50, *Endocrinology and Metabolism Clinics of North America*. W.B. Saunders; 2021. p. 575–90.
37. Horne WC, Shyu JF, Chakraborty M, Baron R. BRIEF REVIEWS Signal Transduction by Calcitonin Multiple Ligands, Receptors, and Signaling Pathways. Vol. 5. 1994.
38. Hsiao CY, Chen TH, Chu TH, Ting YN, Tsai PJ, Shyu JF. Calcitonin Induces Bone Formation by Increasing Expression of Wnt10b in Osteoclasts in Ovariectomy-Induced Osteoporotic Rats. *Front Endocrinol (Lausanne)*. 2020 Sep 8;11.
39. Sabia R, Wagner M, Susa K, Lemke J, Rothermund L, Henne-Bruns D, et al. Calcitonin concentrations in patients with chronic kidney disease on hemodialysis in reference to parathyroidectomy. *BMC Res Notes*. 2019 Jul 19;12(1).
40. Edmonston D, Wolf M. FGF23 at the crossroads of phosphate, iron economy and erythropoiesis. Vol. 16, *Nature Reviews Nephrology*. Nature Research; 2020. p. 7–19.
41. Ho BB, Bergwitz C. FGF23 signalling and physiology. Vol. 66, *Journal of molecular endocrinology*. NLM (Medline); 2021. p. R23–32.
42. Alexander RT, Lee JJ, Plain A, Beggs MR, Dimke H. Effects of phospho- and calciotropic hormones on electrolyte transport in the proximal tubule. Vol. 6, *F1000Research*. Faculty of 1000 Ltd; 2017.
43. Wolf M. Update on fibroblast growth factor 23 in chronic kidney disease. Vol. 82, *Kidney International*. Nature Publishing Group; 2012. p. 737–47.
44. Beggs MR, Alexander RT. Intestinal absorption and renal reabsorption of calcium throughout postnatal development. *Exp Biol Med*. 2017 Apr 1;242(8):840–9.
45. Beggs MR, Young K, Pan W, O'Neill DD, Saurette M, Plain A, et al. Claudin-2 and claudin-12 form independent, complementary pores required to maintain calcium homeostasis. Available from: <https://doi.org/10.1073/pnas.2111247118>
46. Curry JN, Saurette M, Askari M, Pei L, Filla MB, Beggs MR, et al. Claudin-2 deficiency associates with hypercalciuria in mice and human kidney stone disease. *Journal of Clinical Investigation*. 2020 Apr 1;130(4):1948–60.
47. Pan W, Borovac J, Spicer Z, Hoenderop JG, Bindels RJ, Shull GE, et al. The epithelial sodium/proton exchanger, NHE3, is necessary for renal and intestinal calcium (re)absorption. *Am J Physiol Renal Physiol* [Internet]. 2012;302:943–56. Available from: <http://www.ajprenal.org>
48. Rievaj J, Pan W, Cordat E, Todd Alexander R. The Na<sup>+</sup>/H exchanger isoform 3 is required for active paracellular and transcellular Ca<sup>2+</sup> transport across murine cecum. *Am J Physiol Gastrointest Liver Physiol* [Internet]. 2013;305:303–13. Available from: <http://www.ajpgi.org>
49. Alexander RT, Rievaj J, Dimke H. Paracellular calcium transport across renal and intestinal epithelia. In: *Biochemistry and Cell Biology*. National Research Council of Canada; 2014. p. 467–80.
50. Charoenphandhu N, Tudpor K, Pulsook N, Krishnamra N. Chronic metabolic acidosis stimulated transcellular and solvent drag-induced calcium transport in the duodenum of female rats. *Am J Physiol Gastrointest Liver Physiol* [Internet]. 2006;291:446–55. Available from: <http://www.ajpgi.org>

51. Bronner F, Pansu D. Recent Advances in Nutritional Science Nutritional Aspects of Calcium Absorption 1. 1998 Nov 9;
52. Hylander E, Ladefoged K, Jarnum S. Calcium absorption after intestinal resection: The importance of a preserved colon. *Scand J Gastroenterol.* 1990;25(7):705–10.
53. Christakos S, Li S, De La Cruz J, Shroyer NF, Criss ZK, Verzi MP, et al. Vitamin D and the intestine: Review and update. Vol. 196, *Journal of Steroid Biochemistry and Molecular Biology.* Elsevier Ltd; 2020.
54. Beggs MR, Lee JJ, Busch K, Raza A, Dimke H, Weissgerber P, et al. TRPV6 and Cav1.3 Mediate Distal Small Intestine Calcium Absorption Before Weaning. *CMGH.* 2019 Jan 1;8(4):625–42.
55. Kellett GL. Alternative perspective on intestinal calcium absorption: Proposed complementary actions of Cav1.3 and TRPV6. *Nutr Rev.* 2011 Jul;69(7):347–70.
56. Pérez A V., Picotto G, Carpentieri AR, Rivoira MA, Peralta López ME, Tolosa De Talamoni NG. Minireview on regulation of intestinal calcium absorption: Emphasis on molecular mechanisms of transcellular pathway. Vol. 77, *Digestion.* S. Karger AG; 2008. p. 22–34.
57. Lieben L, Benn BS, Ajibade D, Stockmans I, Moermans K, Hediger MA, et al. Trpv6 mediates intestinal calcium absorption during calcium restriction and contributes to bone homeostasis. *Bone.* 2010 Aug;47(2):301–8.
58. Benn BS, Ajibade D, Porta A, Dhawan P, Hediger M, Peng J Bin, et al. Active intestinal calcium transport in the absence of transient receptor potential vanilloid type 6 and calbindin-D9k. *Endocrinology.* 2008 Jun;149(6):3196–205.
59. Lambers TT, Mahieu F, Oancea E, Hoofd L, De Lange F, Mensenkamp AR, et al. Calbindin-D28K dynamically controls TRPV5-mediated Ca<sup>2+</sup> transport. *EMBO Journal.* 2006 Jul 12;25(13):2978–88.
60. Peng JB, Chen XZ, Berger U V, Vassilev PM, Tsukaguchi H, Brown EM, et al. Molecular Cloning and Characterization of a Channel-like Transporter Mediating Intestinal Calcium Absorption\*. 1999; Available from: <http://www.jbc.org>
61. Song Y, Peng X, Porta A, Takanaga H, Peng J Bin, Hediger MA, et al. Calcium transporter 1 and epithelial calcium channel messenger ribonucleic acid are differentially regulated by 1,25 dihydroxyvitamin D<sub>3</sub> in the intestine and kidney of mice. *Endocrinology.* 2003 Sep 1;144(9):3885–94.
62. Ghijsen W, Jong D, Van CO. KINETIC PROPERTIES OF Na<sup>+</sup>/Ca<sup>2+</sup> EXCHANGE IN BASOLATERAL PLASMA MEMBRANES OF RAT SMALL INTESTINE. Vol. 730, *Biochimica et Biophysica Acta.* 1983.
63. Kutuzova GD, Akhter S, Christakos S, Vanhooke J, Kimmel-Jehan C, Deluca HF. Calbindin D 9k knockout mice are indistinguishable from wild-type mice in phenotype and serum calcium level. 2006; Available from: [www.pnas.org/cgi/doi/10.1073/pnas.0605252103](http://www.pnas.org/cgi/doi/10.1073/pnas.0605252103)
64. Airaksinen MS, Eilers J, Garaschuk O, Thoenen H, Konnerth A, Meyer M. Ataxia and altered dendritic calcium signaling in mice carrying a targeted null mutation of the calbindin D28k gene (calcium-binding proteinmotor coordinationsynaptically evoked calcium transientscerebellar Purkinje neuronscalcium imaging) [Internet]. Vol. 94, *Neurobiology.* 1997. Available from: [www.pnas.org](http://www.pnas.org).
65. Ryan ZC, Craig TA, Filoteo AG, Westendorf JJ, Cartwright EJ, Neyses L, et al. Deletion of the intestinal plasma membrane calcium pump, isoform 1, Atp2b1, in mice is associated

- with decreased bone mineral density and impaired responsiveness to 1, 25-dihydroxyvitamin D<sub>3</sub>. *Biochem Biophys Res Commun*. 2015 Nov 6;467(1):152–6.
66. Koushik S V., Wang J, Rogers R, Moskophidis D, Lambert NA, Creazzo TL, et al. Targeted inactivation of the sodium-calcium exchanger (Ncx1) results in the lack of a heartbeat and abnormal myofibrillar organization. *The FASEB Journal*. 2001 May;15(7):1209–11.
  67. Bindels RJM, Ramackers PLM, Dempster JA, Hartog A, Van Os CH. Role of Na<sup>+</sup>/Ca<sup>2+</sup> exchange in transcellular Ca<sup>2+</sup> transport across primary cultures of rabbit kidney collecting system. Vol. 420, *Journal of Physiology*. Springer-Verlag; 1992.
  68. Morgan EL, Mace OJ, Helliwell PA, Affleck J, Kellett GL. A role for Cav1.3 in rat intestinal calcium absorption. *Biochem Biophys Res Commun*. 2003 Dec 12;312(2):487–93.
  69. Li J, Zhao L, Ferries IK, Jiang L, Desta MZ, Yu X, et al. Skeletal phenotype of mice with a null mutation in Cav 1.3 L-type calcium channel. *J Musculoskelet Neuronal Interact*. 2010;10(2):180–7.
  70. Hoenig MP, Zeidel ML. Homeostasis, the milieu inté'rieur, and the wisdom of the nephron. *Clinical Journal of the American Society of Nephrology*. 2014;9(7):1272–81.
  71. Holstein-Rathlou NH, Karlsen FM, Leyssac PP. Blood pressure variability and kidney function. *Fundam Clin Pharmacol*. 1998;12 Suppl 1.
  72. Curry JN, Alan X, Yu SL. Paracellular calcium transport in the proximal tubule and the formation of kidney stones. *Am J Physiol Renal Physiol* [Internet]. 2019;316:966–9. Available from: <http://www.ajprenal.org>
  73. Edwards A, Bonny O. A model of calcium transport and regulation in the proximal tubule. *Am J Physiol Renal Physiol*. 2018 Oct 1;315(4):F942–53.
  74. Downie ML, Alexander RT. Molecular mechanisms altering tubular calcium reabsorption. *Pediatric Nephrology* [Internet]. 2021 Apr 1;37:707–18. Available from: <https://doi.org/10.1007/s00467-021-05049-0>
  75. Yu ASL. Claudins and the kidney. Vol. 26, *Journal of the American Society of Nephrology*. American Society of Nephrology; 2015. p. 11–9.
  76. Ullrich KJ, Rumrich G, Klc S. Active Ca<sup>2+</sup> Reabsorption in the Proximal Tubule of the Rat Kidney Dependence on Sodium-and Buffer Transport. Vol. 364, *Pflügers Arch*. 1976.
  77. Alexander RT, Dimke H, Cordat E. Proximal tubular NHEs: sodium, protons and calcium? *J Physiol Renal Physiol* [Internet]. 2013;305:229–36. Available from: <http://www.ajprenal.org>
  78. Plain A, Pan W, O'neill D, Ure M, Beggs MR, Farhan M, et al. Claudin-12 knockout mice demonstrate reduced proximal tubule calcium permeability. *Int J Mol Sci*. 2020 Mar 2;21(6).
  79. Blaine J, Chonchol M, Levi M. Renal control of calcium, phosphate, and magnesium homeostasis. *Clinical Journal of the American Society of Nephrology*. 2015 Jul 1;10(7):1257–72.
  80. Simon DB, Karet FE, Rodriguez-Soriano J, Hamdan<sup>3</sup> JH, Dipietro<sup>4</sup> A, Trachtmans H, et al. Genetic heterogeneity of Bartter's syndrome revealed by mutations in the K<sup>+</sup> channel, ROMK. *Nature Genetics* [Internet]. 1996;14. Available from: <http://www.nature.com/naturegenetics>
  81. Simon DB, Karet<sup>1</sup> FE, Hamdan JM, Pietro<sup>3</sup> A Di, Sanjad SA, Lifton RP. Bartter's syndrome, hypokalaemic alkalosis with hypercalciuria, is caused by mutations in the Na-

- K-2CI cotransporter NKCC2 . *Nature Genetics* [Internet]. 1996;13:183–8. Available from: <http://www.nature.com/naturegenetics>
82. Hannan FM, Kallay E, Chang W, Brandi ML, Thakker R V. The calcium-sensing receptor in physiology and in calcitropic and noncalcitropic diseases. Vol. 15, *Nature Reviews Endocrinology*. Nature Publishing Group; 2018. p. 33–51.
  83. Lee JJ, Alzamil J, Rehman S, Pan W, Dimke H, Alexander RT. Activation of the calcium sensing receptor increases claudin-14 expression via a PLC -p38-Sp1 pathway. *FASEB Journal*. 2021 Nov 1;35(11).
  84. Dimke H, Desai P, Borovac J, Lau A, Pan W, Todd Alexander R. Activation of the Ca<sup>2+</sup>-sensing receptor increases renal claudin-14 expression and urinary Ca<sup>2+</sup> excretion. Activation of the Ca<sup>2+</sup>-sensing receptor increases renal claudin-14 expression and urinary Ca. *Am J Physiol Renal Physiol* [Internet]. 2013;304:761–9. Available from: <http://www.ajprenal.org>
  85. Hou J, Goodenough DA. Claudin-16 and claudin-19 function in the thick ascending limb. Vol. 19, *Current Opinion in Nephrology and Hypertension*. 2010. p. 483–8.
  86. Hou J, Renigunta A, Gomes AS, Hou M, Paul DL, Waldegger S, et al. Claudin-16 and claudin-19 interaction is required for their assembly into tight junctions and for renal reabsorption of magnesium. *PNAS* September. 2009;8:15350–5.
  87. Jeon US. Kidney and Calcium Homeostasis. *Electrolyte and Blood Pressure* . 2008;6:68–76.
  88. Hoenderop, JGJ, Müller D, Van Der Kemp AWC, Hartog A, Suzuki M, Ishibashi K, et al. Calcitriol Controls the Epithelial Calcium Channel in Kidney. *Journal of the American Society of Nephrology* . 2001;12(7):1342–9.
  89. Hoenderop JGJ, van Leeuwen JPTM, van der Eerden BCJ, Kersten FFJ, van der Kemp AWC, Méritat AM, et al. Renal Ca<sup>2+</sup> wasting, hyperabsorption, and reduced bone thickness in mice lacking TRPV5. *Journal of Clinical Investigation*. 2003 Dec 15;112(12):1906–14.
  90. Khaleel A, Wu MS, Wong HSC, Hsu YW, Chou YH, Chen HY. A single nucleotide polymorphism (rs4236480) in TRPV5 calcium channel gene is associated with stone multiplicity in calcium nephrolithiasis patients. *Mediators Inflamm*. 2015;2015.
  91. Chang Q, Hoefs S, W Van der Kemp A, Topola CN, Bindels RJ, Hoenderop JG. The [beta]-Glucuronidase Klotho Hydrolyzes and Activates the TRPV5 Channel. *Science* . 2005 Oct 21;310(5747).
  92. Singh AK, Saotome K, McGoldrick LL, Sobolevsky AI. Structural bases of TRP channel TRPV6 allosteric modulation by 2-APB. *Nat Commun*. 2018 Dec 1;9(1).
  93. Hoenderop JGJ, Bindels RJM. Calcitropic and magnesiotropic TRP channels. Vol. 23, *Physiology*. 2008. p. 32–40.
  94. Nilius B, Owsianik G, Voets T, Peters JA. Transient Receptor Potential Cation Channels in Disease. *Physiol Rev* [Internet]. 2007; Available from: [www.prv.org](http://www.prv.org)
  95. Hellwig N, Albrecht N, Harteneck C, Schultz G, Schaefer M. Homo- and heteromeric assembly of TRPV channel subunits. *J Cell Sci*. 2005 Mar 1;118(5):917–28.
  96. van Goor MKC, Hoenderop JGJ, van der Wijst J. TRP channels in calcium homeostasis: from hormonal control to structure-function relationship of TRPV5 and TRPV6. Vol. 1864, *Biochimica et Biophysica Acta - Molecular Cell Research*. Elsevier B.V.; 2017. p. 883–93.



97. Hoenderop JGJ, Van Der Kemp AWCM, Hartog A, Van De Graaf SFJ, Van Os CH, Willems PHGM, et al. Molecular identification of the apical  $\text{Ca}^{2+}$  channel in 1,25-dihydroxyvitamin D<sub>3</sub>-responsive epithelia. *Journal of Biological Chemistry*. 1999 Mar 26;274(13):8375–8.
98. Peng J Bin, Chen XZ, Berger U V., Weremowicz S, Morton CC, Vassilev PM, et al. Human calcium transport protein cat1. *Biochem Biophys Res Commun*. 2000 Nov 19;278(2):326–32.
99. Woudenberg-Vrenken TE, Lameris AL, Weißgerber P, Olausson J, Flockerzi V, Bindels RJM, et al. Functional TRPV6 channels are crucial for transepithelial  $\text{Ca}^{2+}$  absorption. *Am J Physiol Gastrointest Liver Physiol* [Internet]. 2012;303:879–85. Available from: <http://www.ajpgi.org>
100. Weissgerber P, Kriebs U, Tsvilovskyy V, Olausson J, Kretz O, Stoerger C, et al. Male Fertility Depends on  $\text{Ca}^{2+}$  Absorption by TRPV6 in Epididymal Epithelia. *Science Signalling* [Internet]. 2011;4(171). Available from: [www.SCIENCESIGNALING.org](http://www.SCIENCESIGNALING.org)
101. Voets T, Janssens A, Prenen J, Droogmans G, Nilius B.  $\text{Mg}^{2+}$ -dependent gating and strong inward rectification of the cation channel TRPV6. *Journal of General Physiology*. 2003 Mar 1;121(3):245–60.
102. Bödding M. Voltage-dependent changes of TRPV6-mediated  $\text{Ca}^{2+}$  currents. *Journal of Biological Chemistry*. 2005 Feb 25;280(8):7022–9.
103. Nilius B, Prenen J, Hoenderop JGJ, Vennekens R, Hoefs S, Freek Weidema A, et al. Fast and slow inactivation kinetics of the  $\text{Ca}^{2+}$  channels ECaC1 and ECaC2 (TRPV5 and TRPV6): Role of the intracellular loop located between transmembrane segments 2 and 3. *Journal of Biological Chemistry*. 2002 Aug 23;277(34):30852–8.
104. Lambers TT, Weidema AF, Nilius B, Hoenderop JGJ, Bindels RJM. Regulation of the mouse epithelial  $\text{Ca}^{2+}$  channel TRPV6 by the  $\text{Ca}^{2+}$ -sensor calmodulin. *Journal of Biological Chemistry*. 2004 Jul 9;279(28):28855–61.
105. Bianco SDC, Peng J Bin, Takanaga H, Suzuki Y, Crescenzi A, Kos CH, et al. Marked disturbance of calcium homeostasis in mice with targeted disruption of the *Trpv6* calcium channel gene. *Journal of Bone and Mineral Research*. 2007 Feb;22(2):274–85.
106. Chen F, Ni B, Yang YO, Ye T, Chen A. Knockout of TRPV6 causes osteopenia in mice by increasing osteoclastic differentiation and activity. *Cellular Physiology and Biochemistry*. 2014;33(3):796–809.
107. Suzuki Y, Kovacs CS, Takanaga H, Peng J Bin, Landowski CP, Hediger MA. Calcium channel TRPV6 is involved in murine maternal-fetal calcium transport. *Journal of Bone and Mineral Research*. 2008 Aug;23(8):1249–56.
108. Khattar V, Wang L, Peng J Bin. Calcium selective channel TRPV6: Structure, function, and implications in health and disease. Vol. 817, *Gene*. Elsevier B.V.; 2022.
109. Nilius B, Vennekens R, Prenen J, Hoenderop JGJ, Droogmans G, Bindels RJM. The single pore residue Asp542 determines  $\text{Ca}^{2+}$  permeation and  $\text{Mg}^{2+}$  block of the epithelial  $\text{Ca}^{2+}$  channel. *Journal of Biological Chemistry*. 2001 Jan 12;276(2):1020–5.
110. Bödding M, Flockerzi V.  $\text{Ca}^{2+}$  dependence of the  $\text{Ca}^{2+}$ -selective TRPV6 channel. *Journal of Biological Chemistry*. 2004 Aug 27;279(35):36546–52.
111. Van der Eerden BCJ, Weissgerber P, Fratzl-Zelman N, Olausson J, Hoenderop JGJ, Schreuders-Koedam M, et al. The transient receptor potential channel TRPV6 is dynamically expressed in bone cells but is not crucial for bone mineralization in mice. *J Cell Physiol*. 2012 May;227(5):1951–9.

112. Neuberger A, Nadezhdin KD, Sobolevsky AI. Structural mechanisms of TRPV6 inhibition by ruthenium red and econazole. *Nat Commun.* 2021 Dec 1;12(1).
113. Oddsson A, Sulem P, Helgason H, Edvardsson VO, Thorleifsson G, Sveinbjörnsson G, et al. Common and rare variants associated with kidney stones and biochemical traits. *Nat Commun.* 2015 Aug 14;6.
114. Yamashita S, Mizumoto H, Sawada H, Suzuki Y, Hata D. TRPV6 gene mutation in a dizygous twin with transient neonatal hyperparathyroidism. *J Endocr Soc.* 2019 Mar 1;3(3):602–6.
115. Zou W Bin, Wang YC, Ren XL, Wang L, Deng SJ, Mao XT, et al. TRPV6 variants confer susceptibility to chronic pancreatitis in the Chinese population. *Hum Mutat.* 2020 Aug 1;41(8):1351–7.
116. Masamune A, Kotani H, Sörgel FL, Chen JM, Hamada S, Sakaguchi R, et al. Variants That Affect Function of Calcium Channel TRPV6 Are Associated With Early-Onset Chronic Pancreatitis. *Gastroenterology.* 2020 May 1;158(6):1626-1641.e8.
117. Walters JRF, Balesaria S, Chavele KM, Taylor V, Berry JL, Khair U, et al. Calcium channel TRPV6 expression in human duodenum: Different relationships to the vitamin D system and aging in men and women. *Journal of Bone and Mineral Research.* 2006 Nov;21(11):1770–7.
118. Xin Y, Malick A, Hu M, Liu C, Batah H, Xu H, et al. Cell-autonomous regulation of epithelial cell quiescence by calcium channel *Trpv6*. *Elife.* 2019 Sep 1;8.
119. Lee GS, Lee KY, Choi KC, Ryu YH, Sang GP, Goo TO, et al. Phenotype of a calbindin-D9k gene knockout is compensated for by the induction of other calcium transporter genes in a mouse model. *Journal of Bone and Mineral Research.* 2007 Dec;22(12):1968–78.
120. Gkika D, Hsu YJ, Van Der Kemp AW, Christakos S, Bindels RJ, Hoenderop JG. Critical role of the epithelial  $\text{Ca}^{2+}$  channel TRPV5 in active  $\text{Ca}^{2+}$  reabsorption as revealed by TRPV5/calbindin-D28K knockout mice. *Journal of the American Society of Nephrology.* 2006 Nov;17(11):3020–7.
121. Zheng W, Xie Y, Li G, Kong J, Feng JQ, Yan CL. Critical role of calbindin-D28k in calcium homeostasis revealed by mice lacking both vitamin D receptor and calbindin-D28k. *Journal of Biological Chemistry.* 2004 Dec 10;279(50):52406–13.
122. Tsukita S, Tanaka H, Tamura A. The Claudins: From Tight Junctions to Biological Systems. Vol. 44, *Trends in Biochemical Sciences.* Elsevier Ltd; 2019. p. 141–52.
123. Günzel D, Yu ASL. CLAUDINS AND THE MODULATION OF TIGHT JUNCTION PERMEABILITY. *Physiological Reviews [Internet].* 2013;525–69. Available from: [www.prv.org](http://www.prv.org)
124. Venugopal S, Anwer S, Szászi K. Claudin-2: Roles beyond permeability functions. Vol. 20, *International Journal of Molecular Sciences.* MDPI AG; 2019.
125. Muto S, Hata M, Taniguchi J, Tsuruoka S, Moriwaki K, Saitou M, et al. Claudin-2-deficient mice are defective in the leaky and cation-selective paracellular permeability properties of renal proximal tubules. *Proc Natl Acad Sci U S A.* 2010 Apr 27;107(17):8011–6.
126. Muto S, Hata M, Taniguchi J, Tsuruoka S, Moriwaki K, Saitou M, et al. Claudin-2-deficient mice are defective in the leaky and cation-selective paracellular permeability properties of renal proximal tubules. *Proc Natl Acad Sci U S A.* 2010 Apr 27;107(17):8011–6.

127. Beggs MR, Appel I, Svenningsen P, Skjødt K, Alexander RT, Dimke XH. Expression of transcellular and paracellular calcium and magnesium transport proteins in renal and intestinal epithelia during lactation. *Am J Physiol Renal Physiol* [Internet]. 2017;313:629–40. Available from: <http://www.ajprenal.org>
128. Tamura A, Hayashi H, Imasato M, Yamazaki Y, Hagiwara A, Wada M, et al. Loss of claudin-15, but not claudin-2, causes Na<sup>+</sup> deficiency and glucose malabsorption in mouse small intestine. *Gastroenterology*. 2011;140(3):913–23.
129. Van De Graaf SFJ, Boullart I, Hoenderop JGJ, Bindels RJM. Regulation of the epithelial Ca<sup>2+</sup> channels TRPV5 and TRPV6 by 1 $\alpha$ ,25-dihydroxy Vitamin D3 and dietary Ca<sup>2+</sup>. In: *Journal of Steroid Biochemistry and Molecular Biology*. 2004. p. 303–8.
130. Hou J, Renigunta A, Gomes AS, Hou M, Paul DL, Waldegger S, et al. Claudin-16 and claudin-19 interaction is required for their assembly into tight junctions and for renal reabsorption of magnesium. Vol. 8, *PNAS* September. 2009.
131. Ashot Kozak J, Putney JW. Calcium Entry Channels in Non-Excitable Cells.
132. Van Abel M, Hoenderop JGJ, Dardenne O, St. Arnaud R, Van Os CH, Van Leeuwen HJPTM, et al. 1,25-Dihydroxyvitamin D3-independent stimulatory effect of estrogen on the expression of ECaCl in the kidney. *Journal of the American Society of Nephrology*. 2002;13(8):2102–9.
133. Hsu YJ, Dimke H, Schoeber JPH, Hsu SC, Lin SH, Chu P, et al. Testosterone increases urinary calcium excretion and inhibits expression of renal calcium transport proteins. *Kidney Int*. 2010 Apr;77(7):601–8.
134. Thongon N, Nakkrasae LI, Thongbunchoo J, Krishnamra N, Charoenphandhu N. Enhancement of calcium transport in Caco-2 monolayer through PKC-dependent Ca v 1.3-mediated transcellular and rectifying paracellular pathways by prolactin. *Am J Physiol Cell Physiol* [Internet]. 2009;296:1373–82. Available from: [www.ajpcell.org](http://www.ajpcell.org)
135. Morgan EL, Mace OJ, Affleck J, Kellett GL. Apical GLUT2 and Cav1.3: Regulation of rat intestinal glucose and calcium absorption. *Journal of Physiology*. 2007 Apr 15;580(2):593–604.
136. Thongon N, Nakkrasae LI, Thongbunchoo J, Krishnamra N, Charoenphandhu N. Enhancement of calcium transport in Caco-2 monolayer through PKC-dependent Ca v 1.3-mediated transcellular and rectifying paracellular pathways by prolactin. *Am J Physiol Cell Physiol* [Internet]. 2009;296:1373–82. Available from: [www.ajpcell.org](http://www.ajpcell.org)
137. Hong EJ, Jeung EB. Biological significance of calbindin-D9k within duodenal epithelium. Vol. 14, *International Journal of Molecular Sciences*. 2013. p. 23330–40.
138. Fujita H, Chiba H, Yokozaki H, Sakai N, Sugimoto K, Wada T, et al. Differential expression and subcellular localization of claudin-7, -8, -12, -13, and -15 along the mouse intestine. *Journal of Histochemistry and Cytochemistry*. 2006 Aug;54(8):933–44.